

RESEARCH

Open Access



NAC1 promotes stemness and regulates myeloid-derived cell status in triple-negative breast cancer

Chrispus Ngule¹, Ruyi Shi^{1,6}, Xingcong Ren¹, Hongyan Jia^{1,7}, Felix Oyelami¹, Dong Li¹, Younhee Park¹, Jinhwan Kim², Hami Hemati¹, Yi Zhang^{1,8}, Xiaofang Xiong³, Andrew Shinkle¹, Nathan L. Vanderford¹, Sara Bachert⁵, Binhua P. Zhou², Jianlong Wang⁴, Jianxun Song^{3*}, Xia Liu^{1*} and Jin-Ming Yang^{1*}

Abstract

Triple negative breast cancer (TNBC) is a particularly lethal breast cancer (BC) subtype driven by cancer stem cells (CSCs) and an immunosuppressive microenvironment. Our study reveals that nucleus accumbens associated protein 1 (NAC1), a member of the BTB/POZ gene family, plays a crucial role in TNBC by maintaining tumor stemness and influencing myeloid-derived suppressor cells (MDSCs). High NAC1 expression correlates with worse TNBC prognosis. NAC1 knockdown reduced CSC markers and tumor cell proliferation, migration, and invasion. Additionally, NAC1 affects oncogenic pathways such as the CD44-JAK1-STAT3 axis and immunosuppressive signals (TGF β , IL-6). Intriguingly, the impact of NAC1 on tumor growth varies with the host immune status, showing diminished tumorigenicity in natural killer (NK) cell-competent mice but increased tumorigenicity in NK cell-deficient ones. This highlights the important role of the host immune system in TNBC progression. In addition, high NAC1 level in MDSCs also supports TNBC stemness. Together, this study implies NAC1 as a promising therapeutic target able to simultaneously eradicate CSCs and mitigate immune evasion.

Keywords TNBC, NAC1, Cancer stem cells, MDSCs, NK cells, TME

*Correspondence:

Jianxun Song
jus35@tamu.edu
Xia Liu
Xia.Liu@uky.edu
Jin-Ming Yang
jyang@uky.edu

¹ Department of Toxicology and Cancer Biology, Department of Pharmacology and Nutritional Science, and Markey Cancer Center, University of Kentucky College of Medicine, Lexington, KY 40536, USA

² Department of Biochemistry, and Markey Cancer Center, University of Kentucky College of Medicine, Lexington, KY 40536, USA

³ Department of Microbial Pathogenesis and Immunology, Texas A&M University Health Science Center, Bryan, TX 77807, USA

⁴ Department of Medicine, Columbia Center for Human Development and Stem Cell Therapies, Columbia University Irving Medical Center, New York, NY 10032, USA

⁵ Department of Pathology and Laboratory Medicine, University of Kentucky, Lexington, KY 40536, USA

⁶ Present Address: Department of Cell Biology and Genetics, Shanxi Medical University, Taiyuan, Shanxi, China

⁷ Present Address: Department of Breast Surgery, First Hospital of Shanxi Medical University, Taiyuan, Shanxi, China

⁸ Present Address: Department of Pharmacology, College of Pharmaceutical Sciences, Soochow University, Suzhou, Jiangsu, China



© The Author(s) 2024. **Open Access** This article is licensed under a Creative Commons Attribution-NonCommercial-NoDerivatives 4.0 International License, which permits any non-commercial use, sharing, distribution and reproduction in any medium or format, as long as you give appropriate credit to the original author(s) and the source, provide a link to the Creative Commons licence, and indicate if you modified the licensed material. You do not have permission under this licence to share adapted material derived from this article or parts of it. The images or other third party material in this article are included in the article's Creative Commons licence, unless indicated otherwise in a credit line to the material. If material is not included in the article's Creative Commons licence and your intended use is not permitted by statutory regulation or exceeds the permitted use, you will need to obtain permission directly from the copyright holder. To view a copy of this licence, visit <http://creativecommons.org/licenses/by-nc-nd/4.0/>.

Introduction

Nucleus accumbens-associated protein 1 (NAC1), encoded by the gene *NAC1* and originally identified as a cocaine-inducible transcript from the nucleus accumbens [1], is a transcription co-regulator that belongs to the BTB/POZ gene family. NAC1 BTB/POZ domain homodimer forms complexes and participates in various biological processes such as transcription regulation, protein degradation, cell proliferation, and apoptosis. NAC1 is important for the pluripotency of embryonic stem cells [2, 3], and can promote mesodermal formation and repress neuroectodermal fate selection in embryonic stem cells via cooperation with other pluripotency transcription factors such as Oct4, Sox2 and Tcf3 [4]. NAC1 knockout mice exhibit a lower survival rate for embryos or newborns, with surviving mice showing defective bony patterning in the vertebral axis [5].

NAC1 was first identified as a cancer-associated gene in ovarian cancer [6], and its overexpression was found in several types of human carcinomas, including ovarian cancer, cervical cancer, colon cancer, and melanoma [6–9]. NAC1 has multifaceted roles in promoting oncogenesis through regulating the expression of a group of genes involved in apoptosis, cell movement, proliferation, Notch signaling, and epithelial-mesenchymal transition [10], and its high expression is associated with tumor growth, survival, and therapy resistance [6, 10–13]. We and others have showed that through its transcription-dependent or -independent functions, NAC1 can inactivate the tumor suppressor Gadd45 [11, 12], promote pro-survival autophagy through the HMGB1-mediated pathway [14], disable cellular senescence [15], bind to actin to regulate cancer cell cytokinesis [16], and induce expression of fatty acid synthase [17]. In the current study, we showed that NAC1 is not only highly expressed in triple negative breast cancer (TNBC), a highly heterogeneous and aggressive form of breast cancer (BC), and supports malignant phenotype of the disease but also contributes critically to the enrichment of cancer stem cells (CSCs), a small subset of cells within tumors and plays crucial roles in driving tumor initiation, metastasis, recurrence, and therapy resistance. The *in vivo* experiments demonstrated that the role of NAC1 in tumor growth and progression is determined by the integrity of the host immune system. Further, we showed that myeloid-derived suppressor cells (MDSCs) with high expression of NAC1 supports stemness of TNBC, and tumoral expression of NAC1 can modulate the functional status of MDSCs and this role of tumor NAC1 is dependent on NK cell status of the host. These findings uncover a novel role of NAC1 in controlling CSCs and MDSCs, two important drivers of tumor progression and immune evasion. Thus, therapeutic targeting of NAC1

to simultaneously eliminate CSCs and reverse immune-suppressive tumor microenvironment (TME) may be exploited as a novel and effective strategy to treatment of highly malignant cancer such as TNBC.

Materials and methods

Retrieval and analysis of bioinformatics data

The pan-cancer breast cancer clinical samples from bioportal which included TCGA, Metabric, Provision and archive datasets [18], were used in this study. Copy number alterations and transcriptome expression of *NAC1* in these datasets were analyzed. The expression patterns of *NAC1* in the basal, luminal, and HER2-positive breast tumors were compared with the normal samples. To determine the protein expression of NAC1 in breast cancer tissues, we utilized UALCAN, an online platform based on TCGA-CPTAC data, which enables the analysis of gene expression profiles in tumor and normal samples [17, 18]. Also, the Timer2.0, a comprehensive platform for systematic analysis of immune infiltrates in tumors (<https://cistrome.shinyapps.io/timer/>, Accessed on: 6–8-2023) [19] was utilized. These computational tools and platforms were employed to gain insights into the expression profiles and clinical implications of *NAC1* in TNBC and their association with immune cell infiltration and tumor immune microenvironment.

Cell lines and culture

Human TNBC cell lines HCC-1806, BT-549, MDA-MB-468, HCC70, and MDA-MB-231, non-TNBC luminal cell lines ZR751 and T47D, and normal epithelial cell line MCF10A, were purchased from the American Type Culture Collection (ATCC); mouse TNBC cell lines 4T1 and EO771 were also from ATCC. MDA-MB-231 and MDA-MB-468 cells were cultured in DMEM medium; HCC1806, ZR751, T47D, HCC70, BT-549, 4T1 and EO771 cell lines were cultured in RPMI-1640 medium. All the cells culture media were supplemented with 10% fetal bovine serum and 1% penicillin–streptomycin. MCF10A was cultured in a mammary epithelial cell growth medium (Promo Cell cat#C201010). Cultured cells were maintained at 37 °C in a humidified atmosphere containing 5% CO₂/95% air. For hypoxic treatment, cells were placed in a hypoxia workstation (Whitley H35 hypohydration, 1% O₂ and 5% CO₂) for 24 h with a continuous nitrogen flow.

Reagents and antibodies

The antibodies used were: GAPDH Mouse mAb (Cell Signaling Technology, #97,166), β -actin antibody (Cell Signaling Technology, #4967), NAC1 (Biolegend, cat#849,302), ADAM17 (Thermo, cat#H00006868-M01A), MMP9 antibody (Santa cruz biotechnology, cat#sc-21733),

MMP1 antibody (Santa cruz biotechnology, cat#sc-21731), CD44 (E7K2Y) XP[®] Rabbit mAb (Cell signaling technology, cat#37,259), CD44-ECD (extracellular domain), anti-human CD44-ICD (intracellular domain) polyclonal antibody (Diagnocine, cat#FNK-KO601), CD24 (Santa Cruz Biotechnology, cat#-sc-19585), Sox2 Rabbit mAb (cell signaling technology, cat#14,962), Nanog (D73G4) XP[®] Rabbit mAb (Cell Signaling Technology, cat#4903), Cyclin D1 (E3P5S) XP[®] Rabbit mAb (Cell Signaling Technology, cat#55,506), ALDH1A1 (Cell Signaling Technology, cat#12,035), STAT3 mouse mAb (Cell Signaling Technology, cat#9139), Phospho-STAT3 (Tyr705) Rabbit mAb (Cell Signaling Technology, cat#9145), JAK1 antibody (Santa Cruz Biotechnology, cat#sc-376996), CD130/gp130 antibody (Santa Cruz Biotechnology, cat#sc-376280), Vimentin Rabbit mAb (Cell signaling technology, cat#5741), mouse anti-E-Cadherin antibody (BD Transduction Laboratories[™], cat#610,181).

Western Blot analysis

Cells were harvested using cold phosphate-buffered saline (PBS) buffer, and the harvested cells were centrifuged to obtain cell pellets. Proteins were extracted from the cell pellets using Laemmli buffer supplemented with protease inhibitor (Peirce protease inhibitor, Thermo Scientific ref#A32963). A BCA assay kit (Pierce BCA protein assay, Thermo Scientific, ref#23,228) was used to quantify the amount of protein. The protein lysate was subjected to sodium dodecyl sulfate–polyacrylamide gel electrophoresis (SDS-PAGE) and then transferred to immun-Blot[®] PVDF (Bio Rad laboratories, ref#1,620,177) membranes for immune-blotting. Following transfer, the membranes were blocked with 5% de-fatted milk for 1 h, followed by overnight incubation with the respective primary antibody at 4 °C. The membranes were washed three times with TBST buffer and then incubated with polyclonal goat anti-rabbit immunoglobulins/HRP (Agilent Dako, cat#P044801-2) or goat anti-mouse immunoglobulins/HRP (affinity isolated) (Agilent Dako, cat#P044701-5) at room temperature for 2 h. Proteins

were visualized using the ChemiDoc[™] MP imaging system (Bio-Rad Laboratories, USA).

Clonogenic assay

Cells (1000 cells/well) were seeded in a 24-well plate and incubated for seven days. At the end of incubation, the cells were fixed with formaldehyde for 15 min, followed by washing with phosphate buffer saline (PBS). The cells were stained with 0.05% crystal violet and the colonies were imaged using the ChemiDoc[™] MP imaging system (Bio Rad, USA).

Immunofluorescence staining

Cells were seeded on coverslips and then placed in a 24-well plate. Twelve hours later, the cells were fixed using 4% paraformaldehyde and permeabilized using 0.2% Triton X-100. Following blocking with 5% bovine serum albumin to minimize non-specific antibody binding, the cells were incubated overnight at 4 °C with respective primary antibodies specific to the target molecules of interest. After the incubation with primary antibodies, cells were thoroughly washed with PBS. Subsequently, fluorochrome-conjugated secondary antibodies were applied to the cells and allowed to bind for 2 h at room temperature. The stained cells were imaged using confocal microscope (Nikon Eclipse Ti2) with suitable filter sets for each fluorochrome.

RNA sequencing and data analysis

Total RNA was extracted using MirVana miRNA isolation kit (Thermo Scientific, Cat#CAM1560, LOT:01126559) and RNA quality and integrity assessed using nanodrop 2000 spectrophotometer (Thermo Scientific, USA). Subsequently, cDNA libraries were generated by reverse transcription of the RNA, followed by double-stranded DNA synthesis. The cDNA libraries were fragmented, and size selection was conducted to obtain fragments within the desired size range. Sequencing-specific adapters were ligated to the cDNA fragments, and PCR amplification was performed to enrich the libraries. The prepared libraries were sequenced

(See figure on next page.)

Fig. 1 High NAC1 expression is associated with tumor progression, stemness, and poor prognosis in TNBC patients. **A** Genetic alterations of NAC1 in breast cancer primary tumors (BPT) in TCGA and Metabric cbiportal datasets. **B** Genetic alterations of NAC1 in breast cancer metastatic tumors (BMT) in archived and provisional cbiportal datasets. **C** Correlation between NAC1 copy number alterations and mRNA expression in TCGA breast cancer patient tissues. **D** Evaluation of NAC1 expression in different stages of breast cancer. **E** NAC1 mRNA expression in TNBC (basal), claudin-low, other breast cancer subtypes (non-TNBC), and normal tissues in Metabric dataset samples. **F** NAC1 copy number alterations in TNBC (basal), other breast cancer subtypes (non-TNBC), and normal tissues in Metabric dataset samples. **G** Western blot of NAC1 expression in TNBC and non-TNBC cell lines. **H** Effect of NAC1 expression on overall survival of patients with TNBC, as analyzed using the TIDE datasets. **I** NAC1 expression in different cell subpopulations at single cell level (Broad Institute single cell portal). **J** Association of NAC1 expression with stemness markers in various cells within the TNBC tumor microenvironment (Broad Institute single cell portal). *n.s.*: not significant; *: $p=0.05$; **: $p=0.01$; ***: $p=0.001$; ****: $p=0.0001$

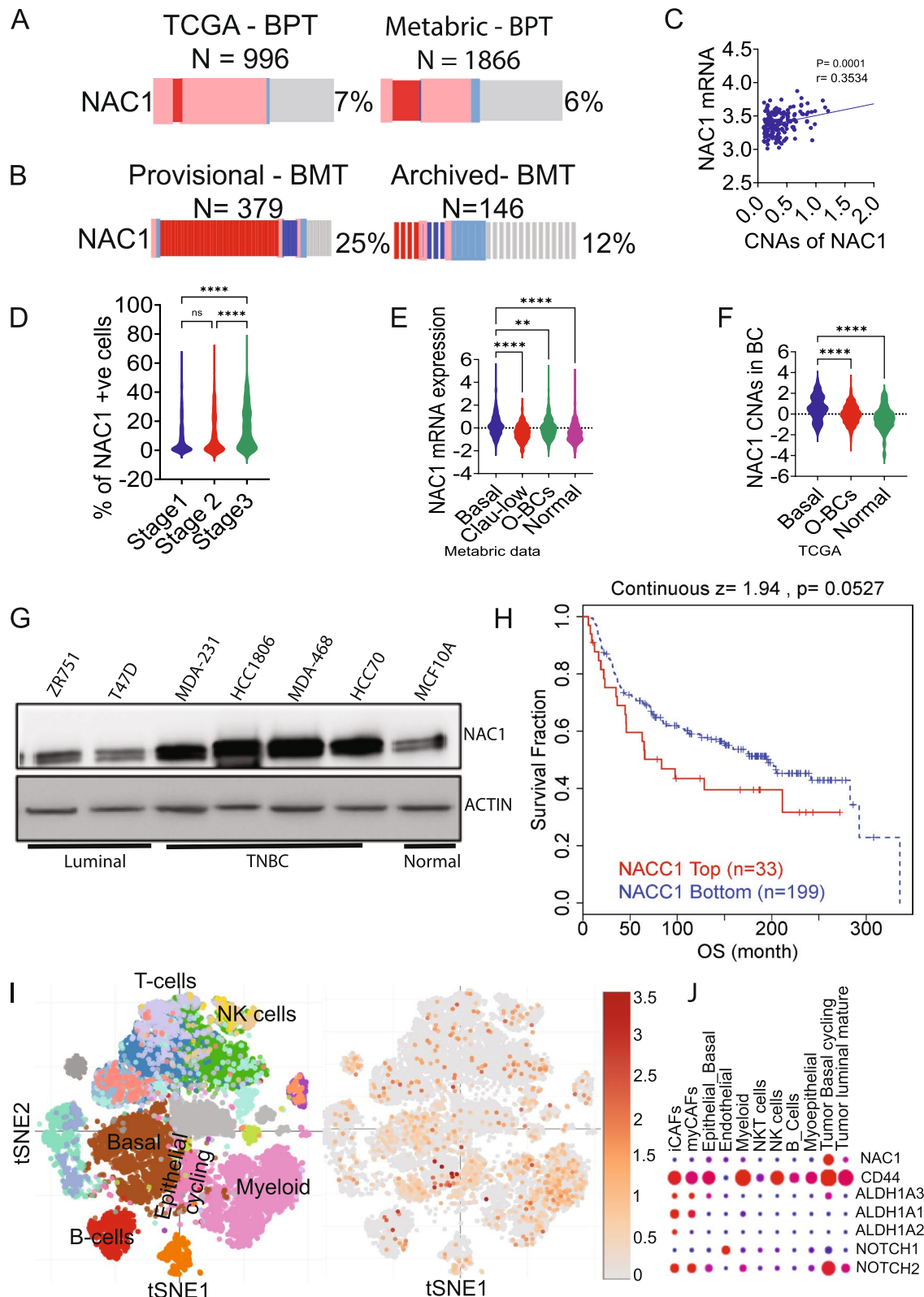


Fig. 1 (See legend on previous page.)

using Illumina sequencing platform (Illumina), and the resulting sequencing data was subjected to bioinformatics analysis, which involved read alignment, transcript assembly, and quantification of gene expression levels using HISAT2 and StringTie. Analysis of differential gene expression was conducted using the DESeq2 analysis tool to determine genes that exhibited significance between the NAC1-deficient and NAC1-expressing cells. Functional annotations and pathway analyses were conducted to gain insights into the biological processes and pathways associated with the differentially expressed genes. BART platform (<http://bartweb.org>) was used to determine the transcription factors (TFs) associated with the differentially expressed genes.

Animal studies

Six-weeks old female NSG mice (NOD.Cg-Prkdcscid Il2rgtm1Wjl/SzJ), Nu/J (nu/nu) mice, BALB/c mice and C57BL/6 J mice were purchased from Jackson Laboratory Bar Harbor, ME USA. NAC1^{-/-} mice were generated by Dr. Jian-Long Wang (Columbia University Irving Medical Center, New York) and crossed in the C57BL/6 background. All the animal experiments were conducted in strict compliance with the regulations of the Institutional Animal Care and Use Committee (IACUC) of University of Kentucky.

For orthotopic tumor inoculation, tumor cells were suspended in 50 μ l of PBS/growth factor-reduced Matrigel (Corning cat#356,255) in a 50/50 ratio and injected into the fat pads of the recipient mice (1×10^6 cells/injection). Nude mice (have active NK cells but lack functional T and B cells) used for MDSC or NK cell depletion were injected with one million cells per mouse in the 2nd and 4th fat pad pairs with a total of 4 tumors (Tn = number of tumors/mice, n = number of mice/group). For tumorigenicity assays, mice were inoculated *s.c.* with different amount of tumor cells (5000, 1000 or 500 cells/inoculation, respectively). For tumor cell lung colonization experiments, tumor cells (1×10^6 cells) were suspended in 50 μ l of PBS and given to mice by tail vein injection and cell homing was monitored by measuring luminescence intensity of the luciferase labeled-cells.

Immunohistochemistry analysis of clinical samples

Formalin-fixed paraffin-embedded (FFPE) tumor resections from breast cancer patients were obtained from the biospecimens core facility of University of Kentucky per the approved Institutional Review Board (IRB) protocol). Immunohistochemistry was performed following the procedures as previously described [20]. Counterstaining was performed with either Mayer's or Harris's hematoxylin. Antibodies used for immunostaining were anti-NAC1, anti-p-STAT3, and anti-Caspase 3. Stained slides were scanned using Aperio slide scanner at 40 \times magnification. Protein expression analysis was performed using halo machine learning software to detect cytosol as well as nucleus protein expression, as previous described [20].

MDSCs and NK cells depletion

To deplete MDSCs in nu/nu mice, animals were administered intraperitoneally with control IgG (mouse IgG2A isotype control, Clone: C1.18.4, Biocell) or anti-Ly6G antibody (anti-mouse Ly6G, Clone: 1A8, Biocell) at a dose of 4 mg/kg/mouse every four days [21] for a period of 20 days. To deplete NK cells in nude mice, anti-NK1.1 antibody (anti-mouse NK1.1, CLONE:PK136, Cat#: BE0036, Biocell) was *i.p.* injected into the recipient mice at a dose of 4 mg/kg/mouse every four days for a period of 20 days [22, 23]. For NK depletion in BALB/C, mice were treated with 25 μ l of anti-Asialo GM1 Polyclonal Antibody (#146,002; clone Poly21460; Biolegend) via *i.p.* injection [24]. Cell depletion efficiency was determined by flow cytometry. Mice were humanely sacrificed on the second day after the last day of antibody treatment.

Isolation of MDSCs from tumor xenografts

Mice were orthotopically inoculated with EO771 cells, and the tumors were allowed to grow for 30 days. Then, the mice were euthanized, and the tumors collected. Tumor tissue digestion was carried out using collagenase-hyaluronidase at 37 $^{\circ}$ C, with shaking at 200 rpm for 30 min. The EasySepTM mouse MDSCs (Gr1⁺/CD11b⁺ cells) isolation kit was used to isolate MDSCs from EO771 tumors obtained from both NACC1^{+/+} or NACC1^{-/-} mice. This kit utilizes negative selection to eliminate other immune and stroma cells. To increase the

(See figure on next page.)

Fig. 2 Effect of NAC1 on stemness of TNBC cells. **A-C** Western blot analysis of the stemness-associated markers in HCC1806 and BT549 TNBC cells with or without knockdown of NAC1. **D** Flow cytometry analysis of CD44 protein surface expression in MDA-MB-231 cells with or without knockdown of NAC1. **E** Flow cytometry analysis of CD24 protein surface expression in MDA-MB-231 cells with or without knockdown of NAC1. **F** *Right*: Mammosphere formation of TNBC cells with or without depletion of NAC1; *Left*: quantification of the number of spheres larger than 45 μ m. **G** Tumor initiation and growth of MDA-MB-231 cells with or without depletion of NAC1 in nu/nu mice. Number of tumors(n) = 2, number of tumors per mouse (Tn) = 4. Luminescence intensity signifies a relative number of detectable live cells

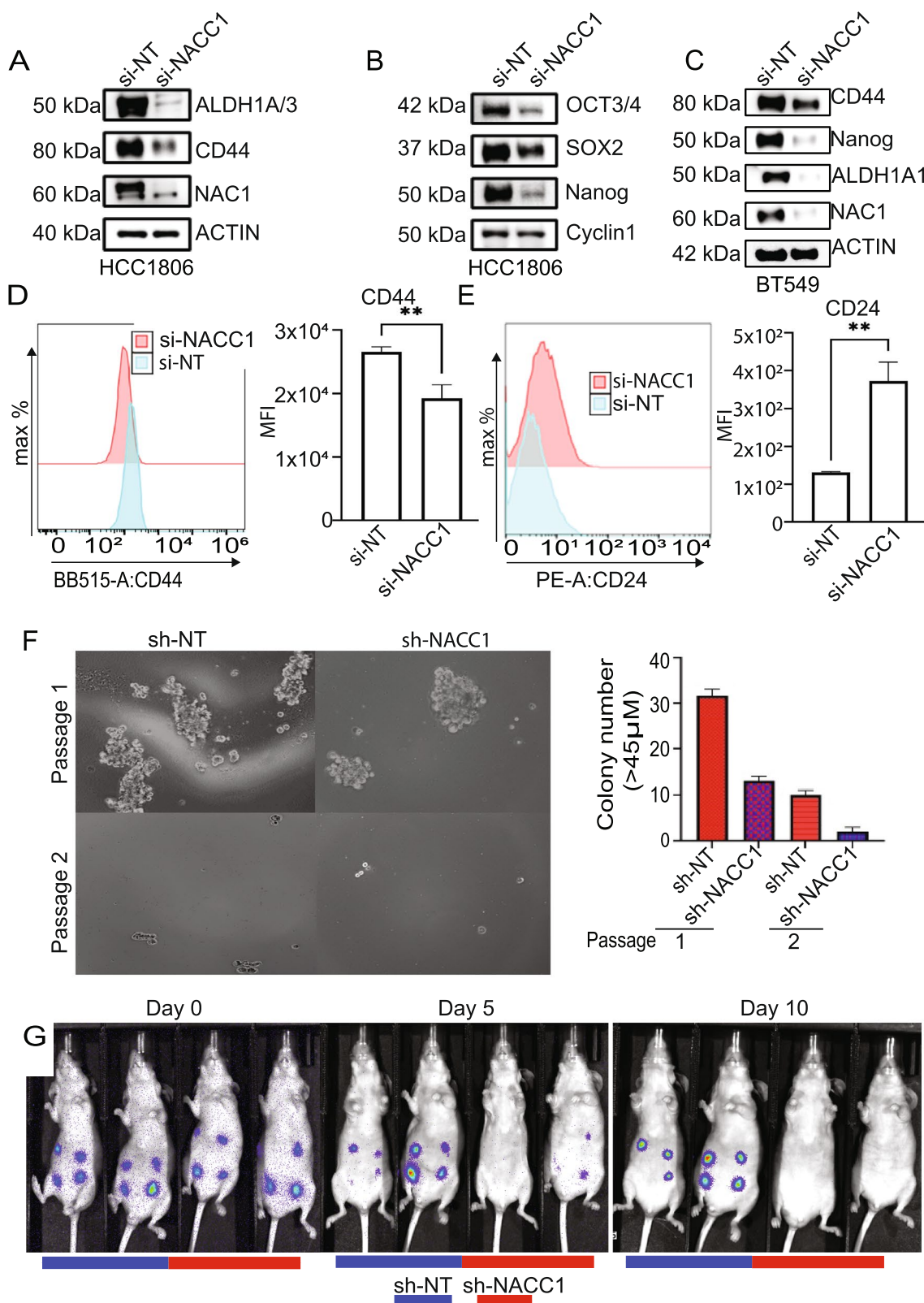


Fig. 2 (See legend on previous page.)

purity of MDSCs and eliminate tumor cell contamination, a CD45 positive selection assay kit (Stem cell technologies, Canada) was utilized.

Statistical analysis

GraphPad Prism software v9.1.2 (www.graphpad.com) was used to perform statistical analyses. Details of specific analysis are presented in the respective legends to figures.

Results

High expression of NAC1 in breast cancer is associated with poor prognosis

In TCGA samples ($N=996$) and Metabric samples ($N=1866$), which are mostly primary tumor tissues, we found that *NAC1* alterations were 7% and 6%, respectively (Fig. 1A), but in the metastatic tumor tissues (cBioportal database), *NAC1* alterations were 25% and 12%, respectively (Fig. 1B). Also, we observed increased *NAC1* deep deletions mainly in breast metastatic tumors (BMT) as compared to breast primary tumors (BPT) (Fig. 1B and Fig. S1A-D), but the role of these deep deletions in tumor progression is unknown. Expression of NAC1 mRNA positively correlated with copy number alterations (CNAs) in breast cancer (Fig. 1C). Accordingly, the expression of NAC1 protein was substantially increased in tumor tissues in comparison to normal tissues (Fig. S2A). NAC1 protein expression was remarkably increased in the breast cancer (BC) tissues harboring alterations in TP53, RB, and c-MYC (Fig. S2B and S2C), the pathways known to be dysregulated in BC. Immunohistochemistry staining and whole slide machine learning analysis of patient tumor specimens from the University of Kentucky tissue bank found increased nuclear expression of NAC1 in stage 3 tumors compared to stage 1 and 2 tumors (Fig. 1D). As BC is a heterogeneous disease and its prognosis differs among different subtypes, we next performed bioinformatic analysis of NAC1 expression in different subtypes of BC. In this analysis, we subdivided the TCGA pan-cancer and Metabric datasets into six molecular subtypes: Luminal A, Luminal B, human epidermal growth factor receptor 2 (HER2), TNBC, claudin expressing tumors, and normal tissues. The

TCGA-pan cancer dataset comprising 1084 samples has 171 basal tissues, 78 HER2-positive, 499 luminal A, 197 luminal B, and 36 normal samples; while the Metabric dataset consists of 2509 samples, including: 209 basal, 218 claudin-low, 224 HER2-positive, 700 luminal A, 475 luminal B, and 148 normal tissues) [18]. Our analysis found that *NAC1* copy number and mRNA expression were increased in the most aggressive basal-subtype samples as compared to other subtypes or normal tissues ($p < 0.05$) (Fig. 1E and F). Additionally, we detected higher NAC1 protein expressions in TNBC cell lines than in luminal or normal epithelial cells (Fig. 1G). In the basal tissue samples but not in other subtypes of BC subtypes, *NAC1* expression was associated with poor prognosis of patients (Fig. 1H and Fig. S3A-C). Additionally, *NAC1* promoter methylation was inversely correlated with the survival of patients with breast cancer (Fig. S3D). Analysis of the TNBC single-cell Broad Institute datasets [25] showed that *NAC1* was not only expressed in tumor cells but also in various immune cells (Fig. 1I). In dividing basal cells, *NAC1* expression positively correlated with the CSC markers CD44, ALDH1A3 and NOTCH2 (Fig. 1J). These results imply that the expression of NAC1 in TNBC may play an important role in driving the malignant phenotype of this disease.

High expression of tumoral NAC1 supports stemness and promotes the malignant phenotype of TNBC

To determine whether there is a causal association between tumoral expression of NAC1 and tumor stemness, we silenced the expression of NAC1 and then examined the expression of CSC markers. Figure 2A-C show that in the NAC1-deficient HCC1806 and BT549 TNBC cells, the expression of CD44, ALDH1A1/2, SOX2, OCT3/4, and NANOG were reduced. Flow cytometry analysis and confocal microscopy imaging revealed a reduced expression of CD44 and increased expression of CD24 in NAC1-knockdown cells (Fig. 2D and E, S3E). Consistently, ALDH1A1/2 activity, a key indicator of CSCs in TNBC, was lower in the tumor cells with depletion of NAC1 than the control cells (Fig. S3F). Furthermore, we show that knockdown of tumoral NAC1 expression reduced the in vitro mammosphere formation

(See figure on next page.)

Fig. 3 Analysis of bulky RNA sequencing data reveals the tumor progression-associated pathways potentially regulated by NAC1. **A** Enrichment of DEGs associated with epithelial-mesenchymal transition (EMT) in MDA-MB-231 cells with deficiency of NAC1. **B** Western blot of metalloproteases in MDA-MB-231 cells with or without depletion of NAC1. **C** Protein expression of EMT-associated marker E-cadherin in MDA-MB-231 cells with or without depletion of NAC1. **D** MDA-MB-231 and BT549 cells subjected to hypoxia show increased NAC1 expression. **E** Gene ontology analysis shows the enrichment of hypoxia, immune regulation, and EMT-associated genes in NAC1-knockdown MDA-MB-231 cells. **F** Expression of hypoxia-associated CA9 gene in MDA-MB-231 cells with or without depletion of NAC1. **G** Expression of vascularization-associated gene VEGFA in MDA-MB-231 cells with or without depletion of NAC1

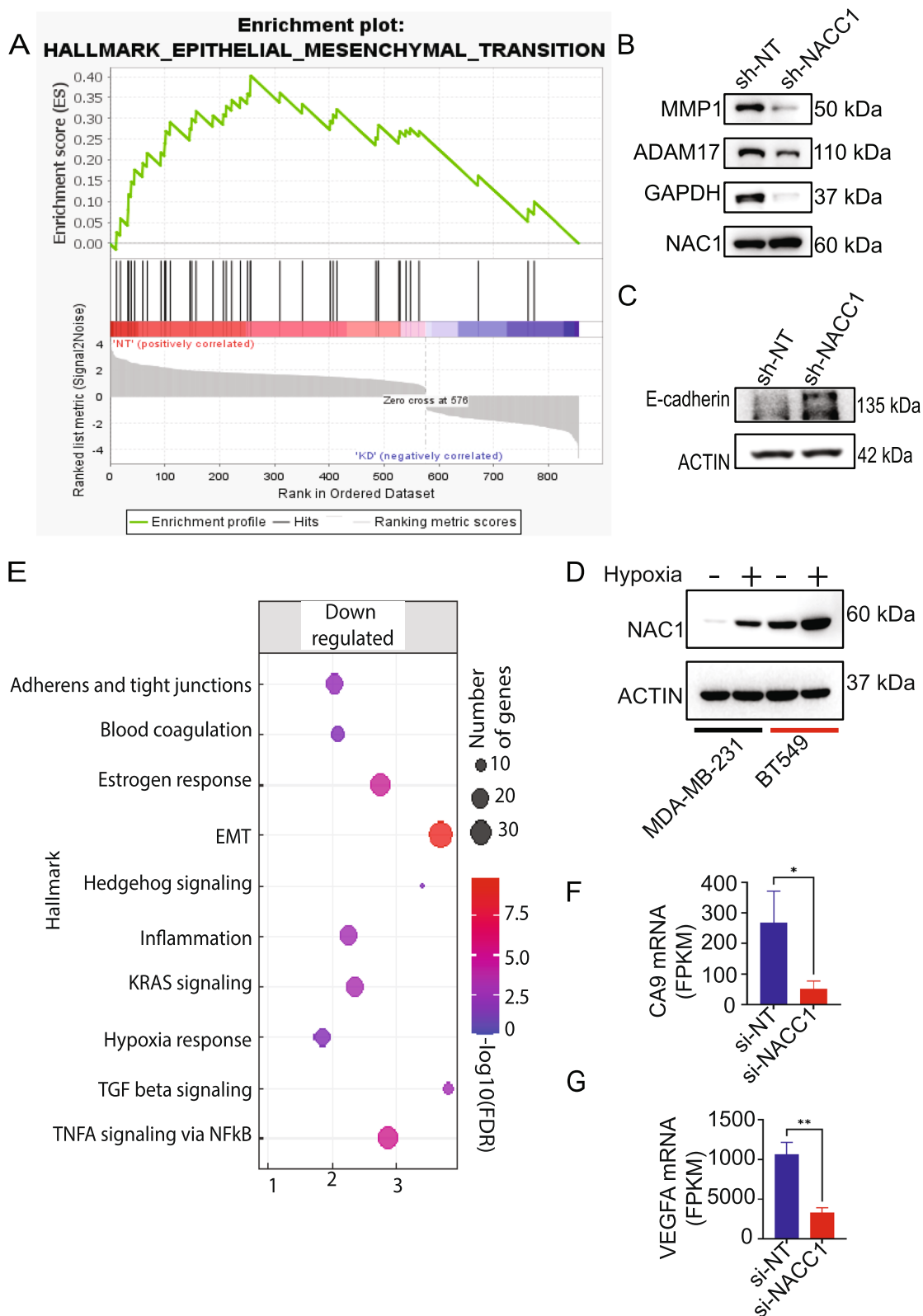


Fig. 3 (See legend on previous page.)

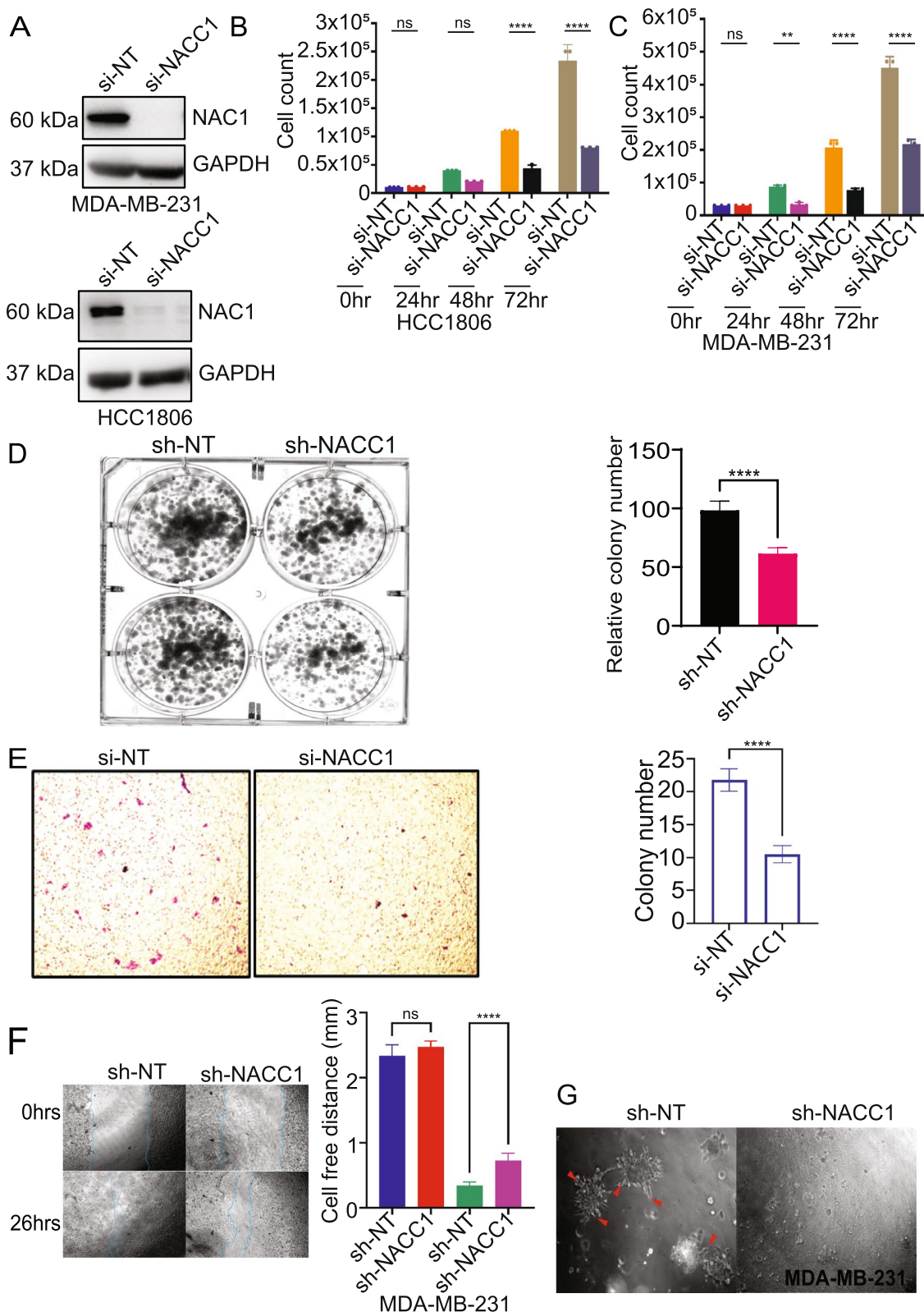


Fig. 4 Effect of NAC1 on proliferation, migration, and invasion of TNBC cells. **A** Western blot of NAC1 in TNBC cells transfected si-NACC1 or si-NT. **B, C** Proliferation of TNBC cells with or without depletion of NAC1. **D** Clonogenic formation of MDA-MB-231 cells with or without depletion of NAC1. **E** Migration of MDA-MB-231 cells with or without depletion of NAC1. **F** Wound healing assay for the migratory ability of MDA-MB-231 cells with or without depletion of NAC1. **G** Matrigel assay for the migratory ability of MDA-MB-231 cells with or without depletion of NAC1

(Fig. 2F) and the in vivo tumorigenicity of the tumor cells (Fig. 2G). These observations suggest that tumoral NAC1 has a role in supporting the enrichment of CSCs.

To further investigate the role of NAC1 in promoting TNBC progression, we performed bulk RNA sequencing analysis on TNBC cells with or without knockdown of NAC1. Our analysis found 856 differentially expressed genes (DEGs) in the NAC1-deficient cells. Out of these DEGs, 576 were downregulated, and 280 were upregulated (adjusted p -value < 0.05, log₂FoldChange > 1) (Fig. S4A). Kyoto Analysis of the Encyclopedia of Genes and Genomes (KEGG) also showed the alterations of some cancer-associated pathways in the NAC1-deficient samples in comparison to the controls (Fig. S4B). Analysis of the sequencing data revealed the enrichment of the genes essential for epithelial-mesenchymal transition (EMT) in tumor cells expressing NAC1 (Fig. 3A), and the downregulations of stemness and EMT-associated genes such as MUC5B family genes, L1CAM, MMP14, MMP1, ADAM17 and SDC4 [26–29] in the NAC1-deficient tumor cells (Fig. 3B, Fig. S4A, Fig. S4C–E). E-cadherin expression increased in the NAC1-deficient tumor cells (Fig. 3C). The tumor stemness marker ALDH1A3, a member of the aldehyde dehydrogenase family and an aldolase uniquely expressed in MDA-MB-231 cells, was significantly downregulated in the NAC1-deficient cells, as compared to the control cells (Fig. S4F). Under hypoxia, cancer stem cells orchestrate the reprogramming of the TME to promote tumor progression [30]. Indeed, the level of NAC1 protein was elevated in the hypoxic tumor cells (Fig. 3D), and the Gene set enrichment analysis (GSEA) showed that the hypoxia response-associated pathways were downregulated in NAC1-deficient TNBC cells (Fig. 3E). Also, the mRNA expressions of the hypoxia marker CA9 and tumor vascularization VEGFA were reduced in the tumor cells deficient in NAC1 (Fig. 3F and G). These data also suggest the role of NAC1 in promoting tumor progression.

Our experiments using MDA-MB-231 and HCC1806 cell lines showed that tumoral expression of NAC1 had

a role in bolstering the proliferation, migration, and invasion of tumor cells. Figure 4A–C show that knockdown of NAC1 expression significantly decreased the proliferation of the tumor cells, reduced their colony formation (Fig. 4D), and inhibited their migration ability (Fig. 4E and F). In addition, the hanging drop assay demonstrated that the sphere size, sphere number and migration ability of the tumor cells subjected to knockdown of NAC1 were significantly decreased (Fig. 4G), suggesting that the expression of NAC1 confers tumor cell resistance to anoikis, a cellular feature that contributes to cancer aggressiveness. Expression of NAC1 in tumor cells also affects their metastatic ability. In C57BL/6 J syngeneic mice, the tail vein injection of NAC1-expressing EO771 tumor cells led to increased lung colonization of tumor cells, but few colonies in the lung were observed in the C57BL/6 J mice injected with the NAC1-deficient EO771 tumor cells (Fig. S5A). The similar difference in lymph nodes metastasis between NAC1-expressing and NAC1-deficient MDA-MB-231 cells was observed in nude mice (Fig. S5B). Additionally, significantly fewer lung metastases were found in NAC1^{-/-} C57BL/6 J mice than in wild-type mice (Fig. S5C–D). Nevertheless, orthotopic injection of NAC1-deficient MDA-MB-231 tumor cells to NSG mice resulted in more tumor cell colonization in the lung, as compared with the injection of the NAC1-expressing cells (Fig. S5E). Because C57BL/6 J, nude and NSG mouse have distinct genetic background and immune system, the discrepancy in tumor cell dissemination observed may be attributed to the difference in the host immune status of these mice.

Activation of STAT3 is involved in the NAC1-mediated oncogenic roles

To explore the molecular mechanism by which NAC1 promotes TNBC progression, we used the BART platform (<http://bartweb.org>) to analyze the transcription factors (TFs) and regulators likely associated with the altered gene expressions through comparing the RNA sequencing data between the tumor cells with or without

(See figure on next page.)

Fig. 5 CD44/JAK-STAT3 is involved in the NAC1-mediated control of TNBC stemness and progression. **A** Analysis of the transcription factors (TFs) associated with the differentially expressed genes in NAC1 knockdown cells demonstrates STAT3 as an important TF in NAC1-induced phenotypes. **B** GSEA analysis demonstrates reduction of genes associated with tumor progression phenotypes and pathways including angiogenesis, cell migration, cell motility and JAK/STAT3 cascade. **C** STAT3 qPCR mRNA analysis of MDA-MB-231 cells. **D** STAT3 mRNA expression in MDA-MB-231 cells with depletion of NAC1. **E** TCGA STAT3 mRNA expression analysis reveals insignificant change ($p > 0.05$) in tumor samples compared to adjacent normal tissues. **F** STAT3 protein expression significantly increases in CPTAC dataset tumor samples compared to normal. **G** Correlation between NAC1, proliferation marker Ki67, caspase 3, and phospho-STAT3 in TNBC patients' tissue from the University of Kentucky retrospective tissue bank. **H** Depletion of NAC1 downregulates STAT3 and phospho-STAT3 protein expression in TNBC cells. **I** JAK1 mRNA expression in MDA-MB-231 cells with depletion of NAC1. **J** Western blot analysis of JAK/STAT3 pathway-associated proteins in MDA-MB-231 cells with depletion of NAC1. **K** CD44 mRNA expression in MDA-MB-231 cells with depletion of NAC1. **L** Depletion of CD44 caused downregulation of JAK1 in MDA-MB-231 cells

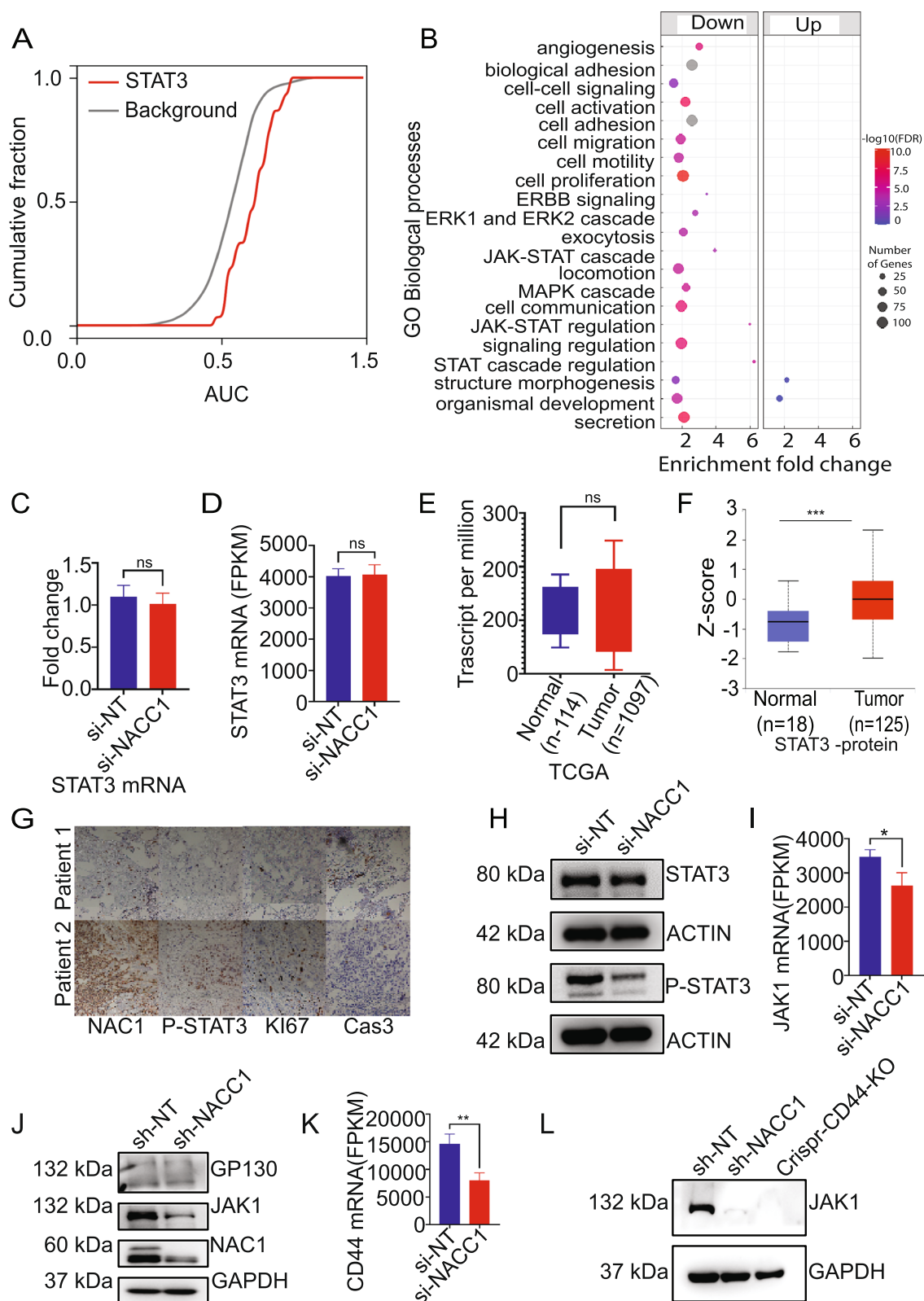


Fig. 5 (See legend on previous page.)

depletion of NAC1. Analysis of TFs found that the downregulated genes associated with loss of NAC1 were strongly associated with STAT3 transcriptional activity ($p < 0.00001$, AUC = 0.74) (Fig. 5A, Fig. S6A), while the upregulated genes were highly associated with chromatin modifier EZH2 ($p < 0.00001$, AUC = 0.842) (Fig. S6B and S6C). These results are consistent with our previous analysis, showing that combining the expressions of both NAC1 and EZH2 in clinical samples could predict the outcome of immunotherapy better than either alone [17].

Comparing the differentially expressed genes in the tumor cells with or without depletion of NAC1 via use of the gene set enrichment analysis (GSEA), we observed reduced expressions of the JAK/STAT pathway-associated genes in the downregulated gene set, as compared to the upregulated gene set in the tumor cells with NAC1 depletion (Fig. 5B). We further analyzed the expression profile of STAT3 transcriptome and protein in the NAC1-deficient tumor cells. We found that the transcription of *STAT3* was similar in the NAC1-deficient cells and control cells, as analyzed by qPCR, RNA sequencing data and UALCAN-TCGA tumor tissue samples ($p > 0.05$) (Fig. 5C, D and E), but STAT3 protein expression increased significantly in the TCGA-tumor samples in comparison to the normal tissues (Fig. 5F). To further interrogate the correlation and clinical relevance of NAC1 protein expression and STAT3 activity, we performed IHC staining for NAC1, phospho-STAT3, proliferation marker Ki67 and apoptosis marker caspase3 in TNBC samples from the tissue bank of University of Kentucky. Figure 5G shows that the level of phospho-STAT3 protein positively correlated with NAC1 and Ki67 expression in TNBC samples; conversely, phospho-STAT3 protein level was negatively correlated with caspase-3 expression. Depletion of NAC1 in TNBC cells caused a reduction of phospho-STAT3 protein and slightly affected the expression of STAT3 (Fig. 5H). These results suggest that NAC1 is involved in activation of STAT3. Analysis of the RNA sequencing data revealed that depletion of NAC1 led to a significant reduction of canonical JAK/STAT3 regulator, JAK1 (Fig. 5I). Protein analysis showed similar results, i.e., depletion of NAC1 led to a reduction in expression of JAK1 (Fig. 5J). Notably, we observed reduced expression

of CD44 mRNA expression in NAC1-deficient tumor cells (Fig. 5K), and CRISPR knockout of CD44 resulted in a decrease of the expression of JAK1 protein, suggesting that CD44 is an upstream regulator of JAK1 (Fig. 5L). These results imply that the CD44-JAK1-STAT3 axis plays a role in the oncogenic function of NAC1 in TNBC.

Expression of tumoral NAC1 is associated with activation of immunosuppressive signaling

As NAC1 showed a role in sustaining tumor stemness (Fig. 2), and CSCs can interact with immune cells in tumor microenvironment (TME) and contribute to immune evasion [31], we next wanted to know whether tumoral expression of NAC1 has any effects on immunosuppressive pathways. Using the gene set enrichment analysis (GSEA), we found the alteration of the genes associated with immune response such as TGF β 1, TGF- α signaling, interferon-gamma and inflammation-associated genes (Fig. 6A), and the downregulations of the innate immunity-associated genes in the NAC1-deficient cells (Fig. 6B). Analysis of the RNA sequencing data showed a decrease of the myeloid-derived cells granulation-linked factors in the NAC1-deficient tumor cells (Fig. 6C). Also, the levels of G-CSF, CCL2, SOD2, and IL6 were downregulated in the NAC1-deficient TNBC cells (Fig. 6D-G). Notably, analysis of gene ontology (GO) enrichment demonstrated the genes associated with secretion pathways, such as secretory granules, secretory vesicles and Golgi apparatus, were downregulated in NAC1 KD cells (Fig. S6D). Since EMT activates the Rab6A-mediated exocytotic process to promote immunosuppressive cytokines secretion in cancer and NAC1 promotes EMT (Fig. 3), we examined the effect of NAC1 on Rab6A. we found that NAC1 deficiency significantly reduced the expression of Rab6A (Fig. S6E). Because IL6 is a major ligand involved in regulation of STAT3 activity and cooperates with G-CSF to polarize myeloid cells towards immunosuppression, we then determined the effect of NAC1 on IL6 expression, using qPCR and enzyme-linked immunosorbent assay. Figure 6F shows that expression of IL6 was significantly decreased in the NAC1-deficient tumor cells. Further, we showed that depletion of tumoral NAC1 led to significant reduction

(See figure on next page.)

Fig. 6 Analysis of bulky RNA sequencing data reveals the immunosuppressive TME-associated factors potentially regulated by NAC1. **A** Altered oncogenic-associated pathways and genes in NAC1-deficient tumor cells. **B** Reactome analysis shows downregulation of innate immunity-associated genes in tumor cells with NAC1 knockdown. **C** Enrichment of the genes associated with neutrophil degranulation in tumor cells with NAC1 knockdown. **D** Expression of G-CSF, CCL2, and SOD2 in MDA-MB-231 cells with or without depletion of NAC1. **E** Expression of CD44 in MDA-MB-231 cells with or without depletion of NAC1. **F** IL6 mRNA expression in MDA-MB-231 cells with or without depletion of NAC1. **G** Level of soluble G-CSF in MDA-MB-231 cells with or without depletion of NAC1. **H** Soluble IL6 concentration in EO771 cells with forced expression of NAC1

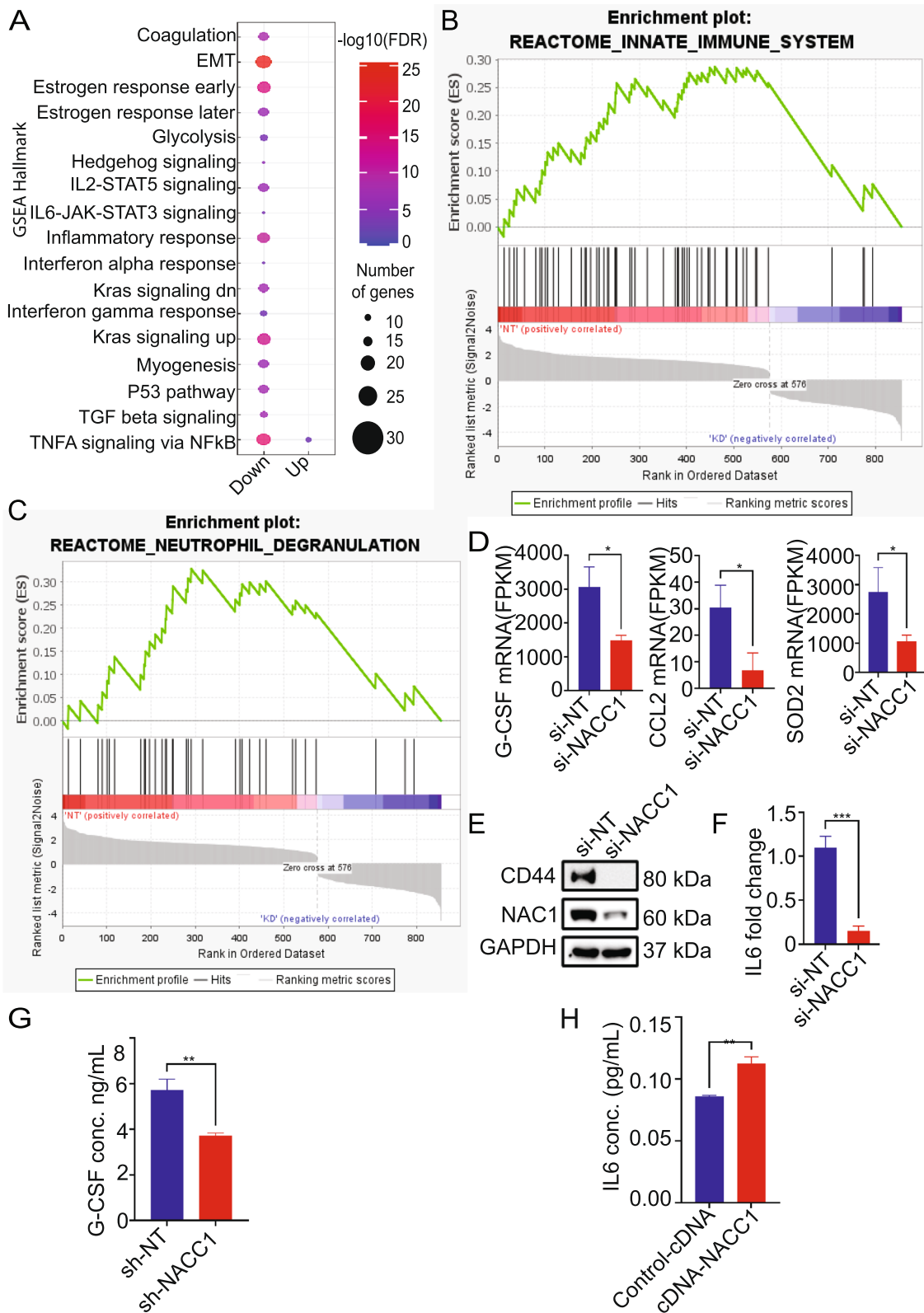


Fig. 6 (See legend on previous page.)

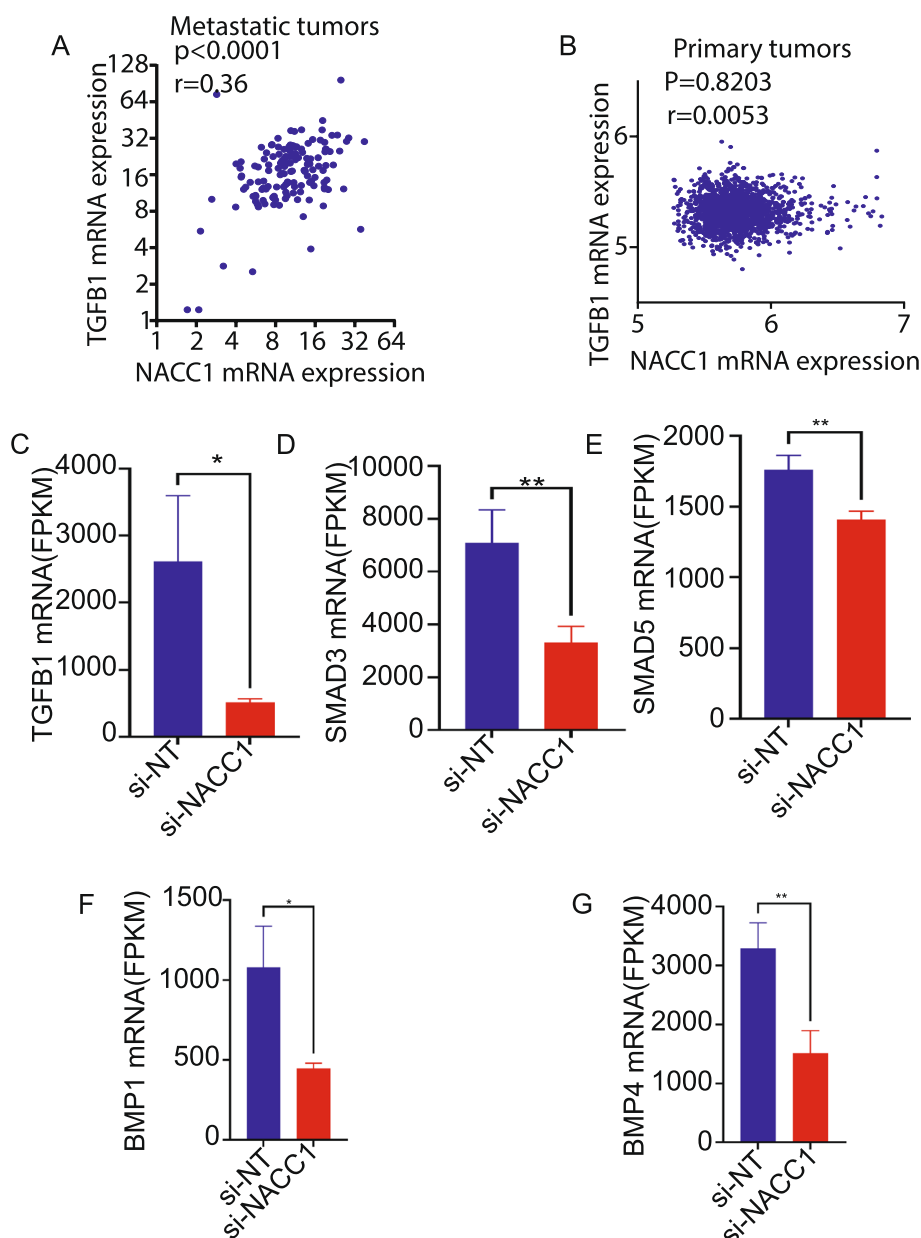


Fig. 7 Effect of NAC1 on TGFβ1 signaling pathway. **A, B** Analysis of the association of NAC1 and TGFβ1 expression using the archived metastatic breast cancer sample dataset (**A**) and using the Metabric breast cancer primary tumor sample dataset (**B**). **C-G** mRNA expressions of TGFβ1 (**C**), SMAD3 (**D**), SMAD5 (**E**), BMP1 (**F**), and BMP4 (**G**) in MDA-MB-231 cells with or without depletion of NAC1

of soluble G-CSF (Fig. 6G). In contrast, EO771 cells subjected to forced expression of NAC1 had a significantly increased amount of soluble IL6 (Fig. 6H). Additionally, analysis of clinical samples showed a positive correlation between NAC1 and TGFβ in metastatic tumor samples (Fig. 7A) but not in the primary tumor tissues (Fig. 7B). The RNA-seq analysis showed that the expressions

of TGFβ1 (Fig. 7C), the TGFβ-interacting proteins SMAD3 and SMAD5 (Fig. 7D and E), and the TGFβ ligands BMP1 and BMP4 were all decreased (Fig. 7F-G) in the tumor cells subjected to knockdown of NAC1. These results suggest that the tumoral NAC1 may have an important role in regulating immunosuppression-associated pathways.

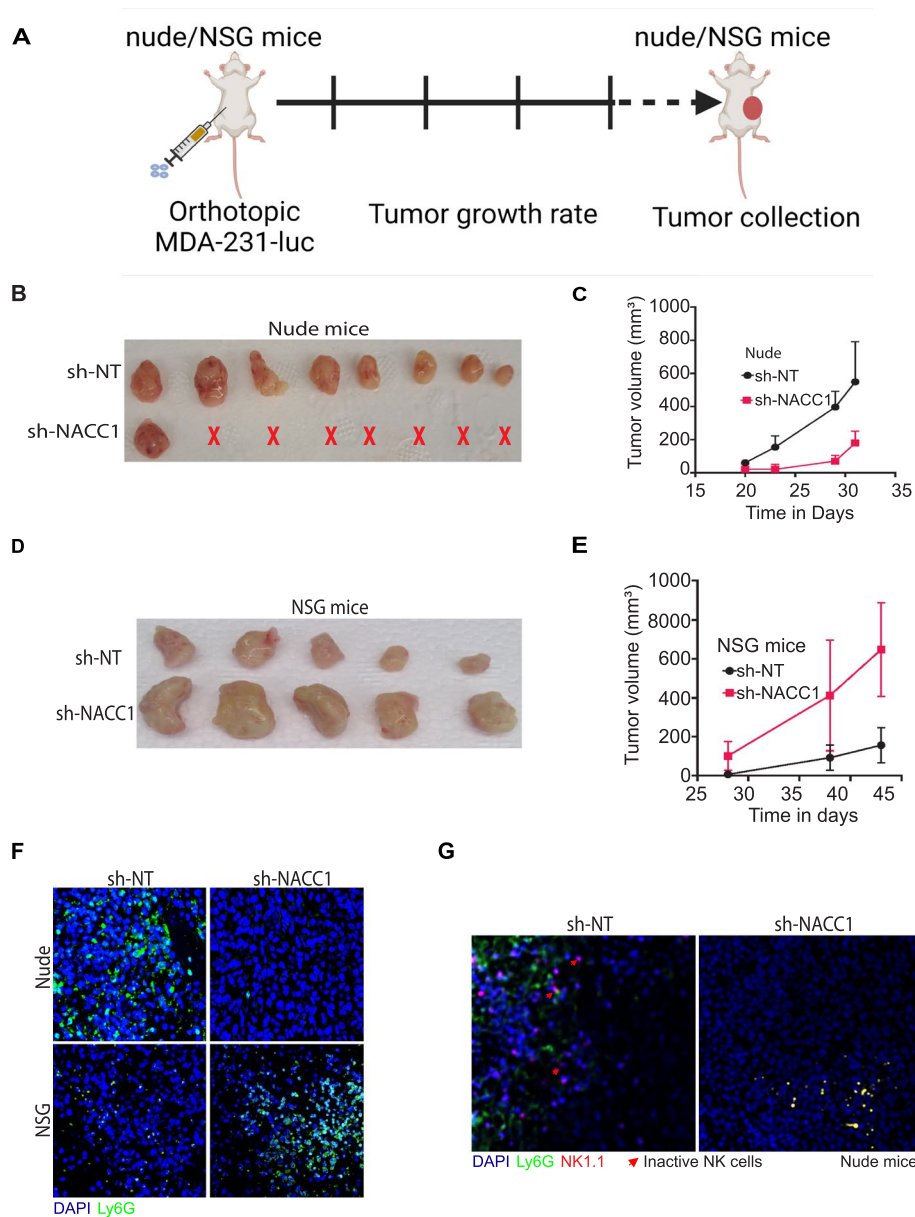


Fig. 8 Comparison of tumor growth of NAC1-expressing and NAC1-deficient TNBC cells in nude or NSG mice ($n=3$, $T_n=2$). **A** Illustration of tumor orthotopic inoculation in nude and NSG mice models. Mice were orthotopically injected with MDA-MB-231 cells (1×10^6 cells/injection, $n=4$, $T_n=2$ on the 4th mammary fat pad) with or without depletion of NAC1, and tumor growth was monitored every five days until mice showed adverse clinical symptoms due to increased tumor burden. **B, C** Tumor growth in nu/nu mice. **D, E** Tumor growth in NSG mice. To evaluate the infiltration of MDSCs and NK cells into the tumor microenvironment, we performed an immunofluorescence assay using Ly6G for MDSCs and NK1.1 and CD16 antibodies for NK cells. **F** Tumor infiltration of MDSCs in the tumor-bearing nude or NSG mice. **G** Tumor infiltration of NK cells in tumor-bearing nude mice, as shown by staining with NK1.1 and CD16 antibodies. Red arrows indicate the inactive NK cells

Role of tumoral NAC1 in tumor initiation and progression is determined by immune status of the host

As NAC1 was shown to contribute to tumor stemness and immunosuppressive pathways including IL6, G-CSE, and TGF-alpha (Figs. 6 and 7) and, both of which can affect tumor development and progression,

we next compared tumor initiation of MDA-MB-231 cells with or without knockdown of NAC1 expression. In these experiments, nude mice or NSG mice were inoculated *s.c.* with tumor cells (1×10^6 cells/mouse), and then the tumor growth was closely monitored (Fig. 8A). Figure 8B, and C show that in NK

cell-competent nude mice, the tumor cells transfected with non-targeting shRNA caused apparent tumor growths; by contrast, the tumor cells subjected to RNAi-mediated depletion of NAC1 barely induced tumor growth. Interestingly, in NSG mice deficient in NK cell we observed that the tumor cells with depletion of NAC1 produced larger tumors than the tumor cells expressing NAC1 (Fig. 8D and E). We further examined and compared the tumor cell proliferation *in vivo* in the nude and NSG mice and observed a similar discrepancy to that of tumor growth (Fig. S7A-B). To explore the cause underlying the different pattern of tumor initiation and development between nude mice and NSG mice, we performed immunofluorescence analyses on MDSCs and NK cells of the resected tumors using the respective marker, as both nude mice and NSG mice possess myeloid derived cells [32]. Figure 8F shows that in nude mice, tumor infiltration of MDSCs was substantially reduced in NAC1 depleted tumors as compared with that in NAC1-expressing tumors; however, in NSG mice, MDSCs infiltration was increased in NAC1 depleted tumors compared with that in NAC1-expressing tumors. Immunofluorescence analyses of NK cells in the tumor specimens from nude mice showed that there were more infiltrations of NK1.1⁺/CD16⁺ double positive cells (mature and activated NK cells) in NAC1-deficient tumors than in NAC1-expressing tumors; NK1.1⁺/CD16⁻ cells, which are inactive NK cells, were detected in the NAC1-expressing tumors but barely detected in the NAC1-deficient tumors (Fig. 8G). Consistent with the observation shown in Fig. 8D and E, the *in vivo* limiting-dilution assay demonstrated that the tumorigenicity of the NAC1-depleted tumor cells in NSG mice was higher than that of the NAC1-expressing tumor cells (Fig. S7C). These observations imply a possible interaction between MDSCs and NK cells in the NAC1-expressing tumors.

Presence or absence of NK cells alters the effect of tumoral NAC1 on MDSCs

To further demonstrate the impact of NAC1 on MDSCs and the influence of NK cells, we depleted myeloid cells or NK cells of nude mice using Ly6G antibody and NK1.1 antibody, respectively, and then monitored tumor growth in mice inoculated with MDA-MB-231 cells with or without depletion of NAC1 (Fig. 9A and Fig. S7D). Consistent with what we observed in NSG mice (Fig. 8D and E), in the nude mice depleted of NK cells, NAC1-depleted tumor cells exhibited a substantially enhanced tumorigenicity as compared with the control tumor cells (Fig. 9B-F); and depletion of myeloid cells (Fig. 9G) caused a decreased growth of NAC1-expressing tumors but led to an enhanced growth of NAC1-depleted tumors in nude mice (Fig. 9H-L). These results demonstrate that in the presence of tumor NAC1, myeloid-derived cells have negative effect on NK cells, and loss of NAC1 decreases the tumor-promoting activity of MDSCs but increases the tumor-inhibiting activity of MDSCs as well as NK cells. When NK cells are depleted, the NAC1-expressing and NAC1-depleted tumor cells both show enhanced tumorigenicity; however, when myeloid-derived cells are deprived, the tumorigenicity of NAC1-expressing cells is reduced, but NAC1-deficient tumor cells show enhanced tumor growth, suggesting that absence of the tumor-inhibiting myeloid-derived cells may diminish the activity of NK cells in NAC1-depleted tumors. These results indicate that the effect of NAC1 on myeloid-derived cells is NK cell-dependent and were also observed in immunocompetent BALB/C mice bearing knockdown 4T1 wells. In this model, we showed that knockdown of NAC1 lead to a significant decrease in tumor growth, and this could be rescued by depletion of NK cells in these mice (Fig. 10A, Fig. S8A-C). These observations support a role of innate immune cells in antitumor immunity.

(See figure on next page.)

Fig. 9 Effects of NK cells on growth of NAC1-expressing and NAC1-deficient TNBC cells in nude mice. **A** Illustration of NK cell depletion approach. Mice were orthotopically inoculated with the luciferase plasmid transfected-MDA-MB-231 cells with or without depletion of NAC1 (1×10^6 cells/inoculation, $n=4$, $T_n=4$). On day four following tumor inoculation, the mice were given NK1.1 antibody or control IgG (4 mg/kg) intraperitoneally five times with a four day-interval to deplete NK cells. Tumor cell proliferation and tumor growth were monitored using the Lago optical imaging system. **B, C** Luminescence intensity of tumor cells grown in mice with or without NK cell depletion (**B**) and quantification of the luminescence intensity (photon emission) (**C**). **D** Tumor volume (mm^3) in mice with or without NK cell depletion. **E** Tumor formations in the mice treated with NK1.1 antibody or IgG. **F** Tumor weights in mice with or without depletion of NK cells. **G** Illustration of MDSCs depletion approach. Mice were orthotopically inoculated with the luciferase plasmid transfected-MDA-MB-231 cells (1×10^6 cells/inoculation, $n=2$, $T_n=4$) with or without depletion of NAC1. On day four following tumor inoculation, the mice were given Ly6G antibody or control IgG (4 mg/kg) intraperitoneally five times with a four day-interval to deplete MDSCs. Tumor cell proliferation and tumor growth were monitored using the Lago optical imaging system. **H, I** Luminescence intensity of tumor cells grown in mice with or without depletion of MDSCs (**H**) and quantification of the luminescence intensity (photon emission) obtained on the last day of antibody depletion treatment. **J** Tumor volume (mm^3) in mice with or without depletion of MDSCs. **K** Tumor formations in the mice treated with Ly6G antibody or IgG. **L** Tumor weights in mice with or without depletion of MDSCs

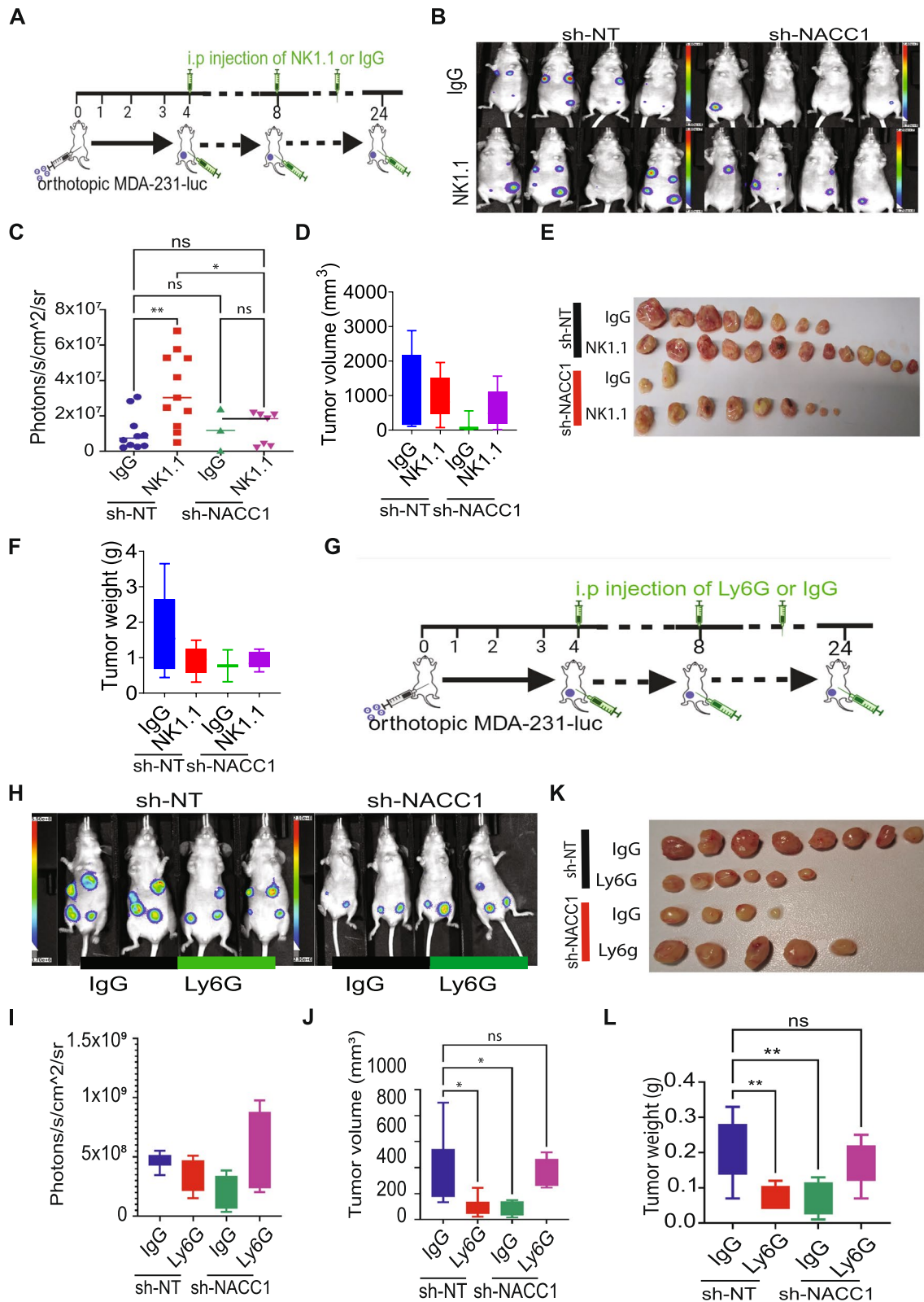


Fig. 9 (See legend on previous page.)

Also, as deficiency of tumoral NAC1 caused downregulation of IL6, G-CSF, and TGF β 1 (Figs. 6 and 7), all of which have immunosuppressive effects, NAC1 may control the status of MDSCs through modulating the levels of these cytokines, thereby impacting tumor initiation and development.

MDSCs with high expression of NAC1 support stemness of TNBC

Next, we determined the expression of NAC1 in MDSCs and its effect on CSCs, as the interaction of immune cells with CSCs in TME has crucial roles in tumor growth and metastasis [33, 34]. We inoculated BALB/c mice with 4T1 tumor cells and then compared NAC1 expression in MDSCs from tumor-bearing mice with that in MDSCs from tumor-free mice. Figure 10B shows that in addition to the high level of NAC1 in the tumor infiltrated MDSCs, NAC1 was also up-regulated in MDSCs from the spleen, blood, and bone marrow of the tumor-bearing mice, compared with those from the tumor-free animals. To assess the effect of NAC1 in MDSCs on their activity, we co-cultured EO771 tumor cells with MDSCs from the wild-type mice or NAC1 knock-out mice (Fig. 10C), then analyzed and compared the levels of CD44 and aldolase activity in the tumor cells. Figures 10D and E show that CD44 expression and aldolase activity in the EO771 tumor cells co-cultured with Gr1⁺/CD11b⁺ cells from NAC1^{-/-} mice were reduced, as compared with that in the EO771 cells co-cultured with Gr1⁺/CD11b⁺ cells from the wild-type mice, suggesting a role of NAC1-expressing MDSCs in maintaining CSCs. Also, the tumor initiation of EO771 cells was lower in NAC1^{-/-} C57BL/6 J mice than that in wild-type mice (Fig. 10F). These results imply that NAC1 expression in MDSCs affects their tumor-promoting function as well as tumor stemness. Additionally, Gr1⁺/CD11b⁺ cells from the tumor-bearing NAC1^{-/-} C57BL/6 J mice showed stronger cytotoxic effect than those from wild-type mice when co-cultured with tumor cells (Fig. 10G-I), suggesting that expression of NAC1 in MDSCs controls their tumor-inhibitory or tumor-promotive activity.

Discussion

We recently identified a NAC1-regulated gene signature in TNBC, and this gene signature includes several CSC-associated genes [35]. To pursue these findings, in this study we tested our hypothesis that expression of NAC1 in TNBC plays a critical role in driving its malignant phenotype via supporting enrichment of CSCs, a small subset of cancer cells that possess stem cell-like properties [36, 37] and one of the major contributors to the tumor heterogeneity and tumor initiation, metastasis, and resistance to therapy [38–42, 43]. The results of this study show that high expression of NAC1 in TNBC bolsters stemness and contributes to development and progression of this neoplasm, and this important role involves the activation of STAT3 pathway. We also demonstrate that tumoral expression of NAC1 plays a role in activating the immunosuppressive signals such as TGF-beta IL6 and G-CSF, and in controlling interaction between CSCs and cancer-associated MDSCs. Remarkably, the effect of NAC1 on tumor growth and progression appears to be dictated by the status of NK cells and MDSCs, and MDSCs with high expression of NAC1 show a supportive role in maintaining the stemness of TNBC. Although the previous studies including our own have demonstrated the high expression of NAC1 in various cancers and its involvement in oncogenesis and therapy resistance [6, 14, 35, 44, 45], whether NAC1 has roles in regulating CSCs and immune-TME, the two key independent but highly related factors that contribute critically to cancer development and progression, have been unexplored. A better understanding of the key drivers of CSCs and immunosuppressive TME may help develop novel and effective therapeutic intervention for metastatic malignancies such as TNBC.

There are studies showing that NAC1 participates in regulation of self-renewal and pluripotency of embryonic stem cells [2, 3, 46] and somatic cell reprogramming by controlling the expressions of Zeb1 and E-cadherin [47]. Here, we demonstrate the promotive effects of NAC1 on the expressions of stemness markers of breast cancer, CD44, CD24, and ALDH1, and on several BCSC (breast cancer stem cells)-associated features, including tumor growth and metastasis, providing new insights

(See figure on next page.)

Fig. 10 Myeloid-derived cells with expression of NAC1 supports CSCs. **A** Tumor growth rate for knockdown 4T1 allografted cells with or without NK cell depletion. **B** Expression of NAC1 in MDSCs from 4T1 tumor-bearing or tumor-free BALB/C mice. **C** Gr1⁺/CD11b⁺ cells were isolated from the NAC1^{+/+} or NAC1^{-/-} mice bearing EO771 tumors through negative selection to obtain MDSCs and were further purified using CD45 positive selection assay kit (Stemcell technologies) to eliminate contaminating tumor cells. **D** EO771 cells co-cultured with NAC1^{-/-} Gr1⁺/CD11b⁺ cells showed reduced CD44 expression compared to the co-culture with NAC1^{+/+} Gr1⁺/CD11b⁺ cells. **E** Aldolase activity of EO771 cells co-cultured with NAC1^{+/+} or NAC1^{-/-} mice Gr1⁺/CD11b⁺ cells. **F** Tumor initiation ability of EO771 cells orthotopically inoculated in NAC1^{+/+} or NAC1^{-/-} mice ($n=5$, $Tn=2$). **G-I** EO771 cells were co-cultured with NAC1^{+/+} or NAC1^{-/-} Gr1⁺/CD11b⁺ cells, and cell viability was determined using the CellTrace™ CFSE Cell Proliferation Kit (**G**) or Luciferase assay (**H**)

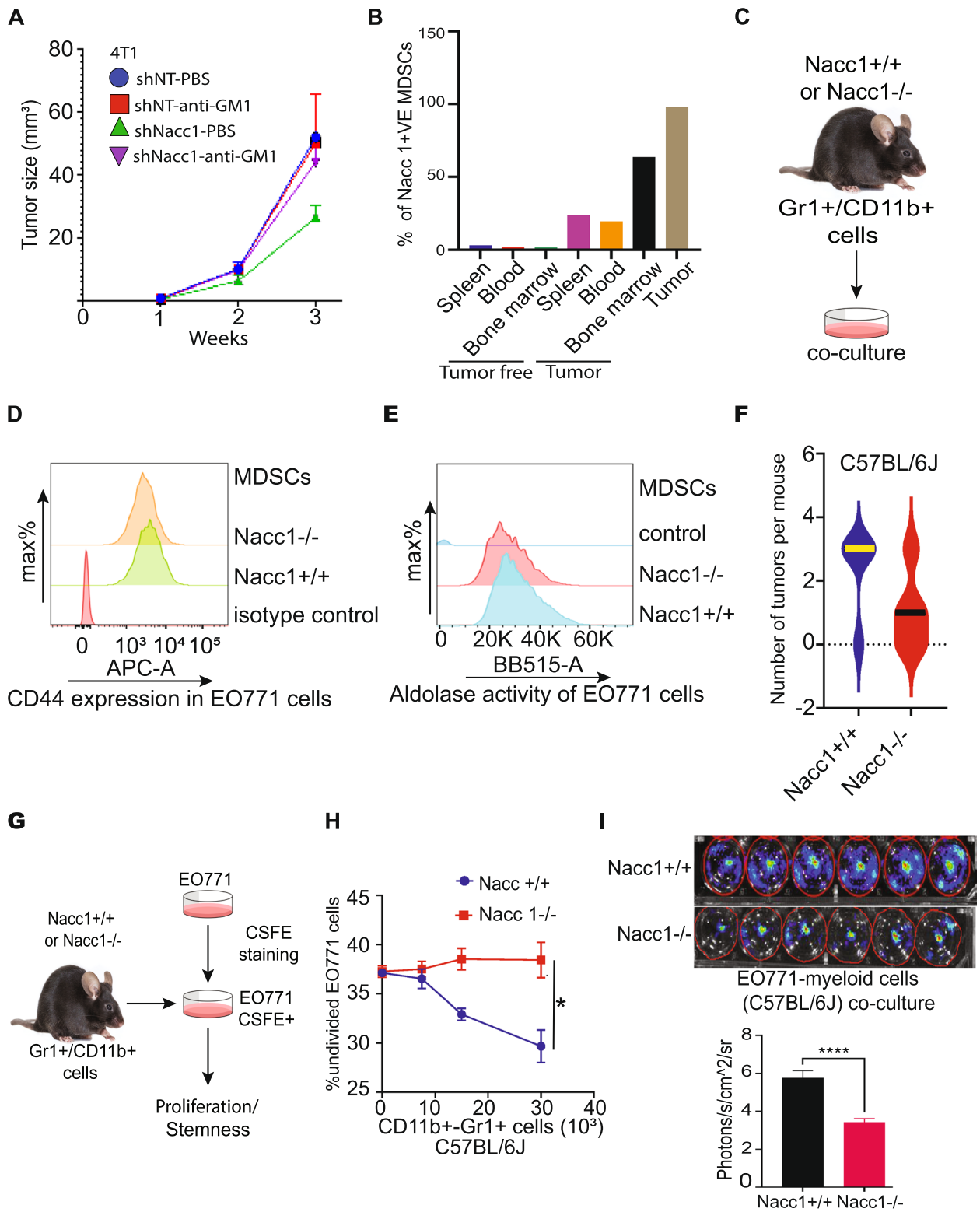


Fig. 10 (See legend on previous page.)

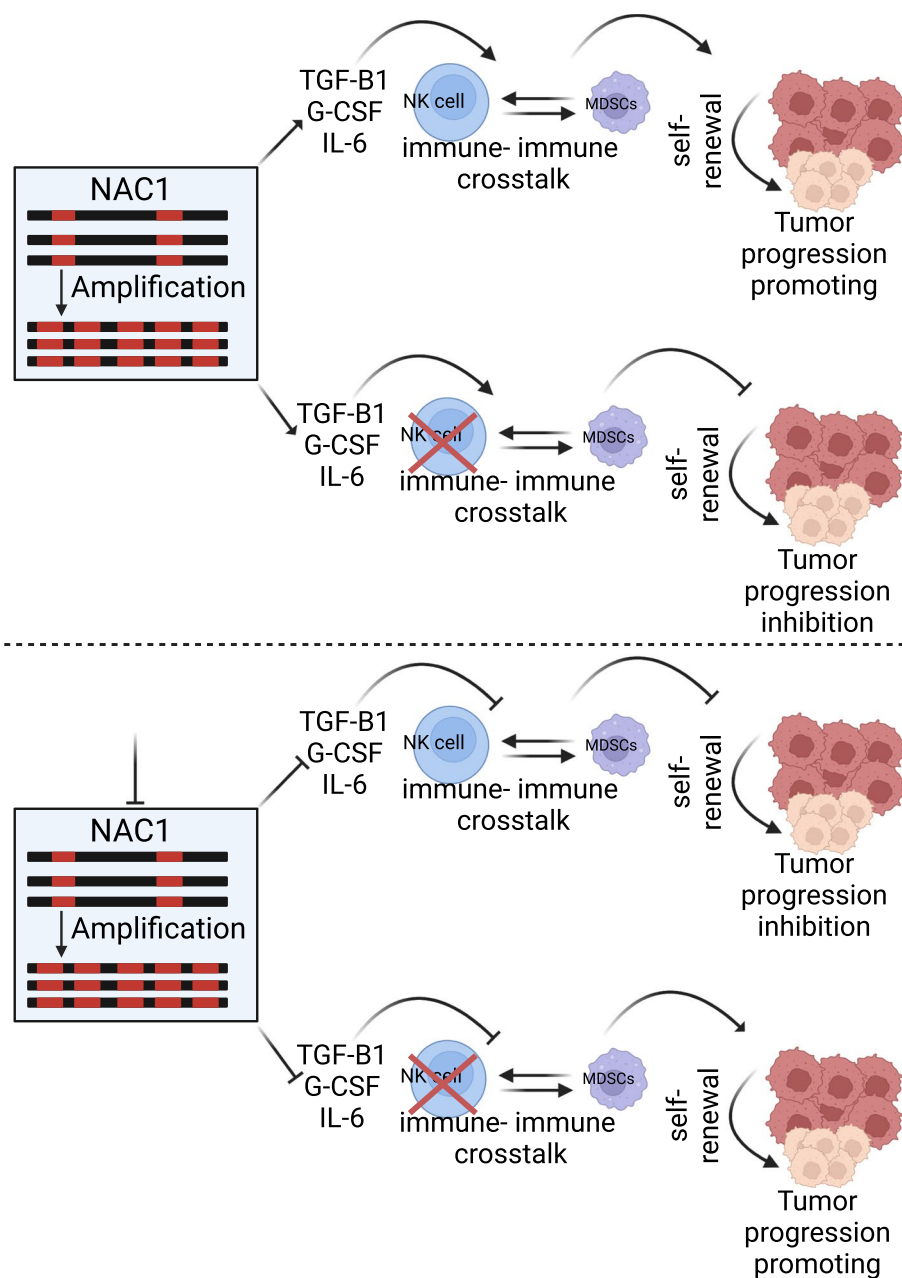


Fig. 11 Proposed model. High expression of NAC1 in TNBC promotes tumor stemness and induces secretion of immunosuppressive cytokines, which orchestrate tumor infiltration of MDSCs and NK cells and tumor stemness. MDSCs support stemness properties and aid tumor immune evasion, promoting tumor growth and progression

into the biological functions of NAC1. We also show that NAC1 can modulate the JAK1-STAT3 axis via CD44, which may be responsible for the role of NAC1 in TNBC progression. These results are in line with a previous study showing that the intracellular domain of CD44 can bind and stabilize STAT3 to enhance its transcriptional activity [48]. Emerging evidence has revealed that enrichment of CSCs not only directly contributes to the

malignant phenotype of TNBC [49–51] but also shapes immunosuppressive TME via interaction with immune cells to sustain their stem cell states, leading to immune evasion and progression of the disease [52]. Interestingly, although we show that expression of NAC1 favors CSC enrichment, the effect of NAC1 on tumor development and progression is strikingly different in NK cell-competent nude mice and NK cell-deficient NSG mice: in nude

mice, depletion of tumoral NAC1 reduced tumor growth and inhibited tumor metastasis; but in NSG mice, depletion of tumoral NAC1 promoted tumor growth and metastasis. Further, we observed in nude mice that the NAC1-deficient tumors had much less MDSC accumulation than the NAC1-expressing tumors; oppositely, in NSG mice, the NAC1-deficient tumors recruited much more MDSCs than the NAC1-expressing tumors. On the other hand, the tumors with depletion of NAC1 showed more infiltration of matured and activated NK cells than the tumors with NAC1 expression. These observations imply that tumoral expression of NAC1 negatively affects antitumor immune response by promoting the activity of immune-suppressive cells and inhibiting tumor-killing immune cells in the host that has both MDSCs and NK cells. Moreover, NK cells can modulate the effect of NAC1 on MDSCs. Control of the tumor-modulating role of MDSCs (tumor-associated neutrophils) by the host NK cell status has also been found in murine breast cancer models by Ren's group [23]. More recently, it was reported that TME has a critical role in regulating neutrophils [53]. Nevertheless, whether myeloid-derived cells, including neutrophils, are pro- or anti-tumorigenic and how their dual roles are regulated remain to be further elucidated [23, 54]. Despite the emerging evidence showing that high-stemness signature correlates with poor immune response in solid neoplasms [55] and that CSCs can recondition MDSCs and shape immunosuppressive TME to sustain their stem cell states, causing immune evasion and the malignant phenotype of CSCs [31, 52, 56], whether the effects of NAC1 on these immune cells, as observed in this study, are due to the presence of CSCs or the cytokines (e.g., TGF- β or IL6) produced by the NAC1-expressing tumors would need further investigation. Also, we show that MDSCs $NAC1^{+/+}$ uphold tumor cell proliferation as well as tumor stemness, but the myeloid-derived cells from the tumors grown in mice $NAC1^{-/-}$ are more cytotoxic than that from the tumors grown in mice $NAC1^{+/+}$, implying a possible symbiosis or NAC1-governed cross-talk between MDSCs and CSCs in TME, and this interaction might be controlled by the signaling that can simultaneously affect the maintenance of CSCs and activity immune-suppressive cells (e.g., TGF- β , STAT3, G-CSF). Indeed, we found that the expressions of TGF- β , STAT3, G-CSF, and IL-6 are reduced in tumor cells deficient in NAC1. In addition, because accumulation of MDSCs such as G-MDSCs is one of the causes for anti-PD1 therapy resistance [57–64], it would be interesting to test whether targeting NAC1 could improve the efficacy of cancer immunotherapy such as immune checkpoint inhibitors.

Conclusions

This study identified NAC1 as a critical determinant that not only promotes tumor stemness but also contributes to immunosuppressive TME. The complex role of NAC1 in TNBC progression is determined by the integrity of the host immune system. In the absence of host's NK cells, NAC1 acts as a tumor suppressor while in the presence of host's NK cells, depletion of NAC1 shows oncogenic role of this protein (Fig. 11). As the chemotherapy-induced toxicity often involves alterations of immune cells, including NK cells and various myeloid-derived cells [23, 65], whether targeting of NAC1 has advantage or disadvantage in treatment of patients with TNBC and receiving other therapies might depend on the host immune status (Fig. 11). The potential of NAC1 as a novel therapeutic target able to simultaneously eliminate CSCs and mitigate immune-suppressive TME warrants further investigation.

Abbreviations

ATCC	American Type Culture Collection
BART	Binding Analysis for Regulation of Transcription
BC	Breast cancer
BCA	Bicinchoninic Acid
BCSC	Breast Cancer Stem Cells
CPTAC	Clinical Proteomic Tumor Analysis Consortium
CRISPR	Clustered Regularly Interspaced Short Palindromic Repeats
CSC	Cancer Stem Cells
DEGs	Differentially expressed genes
EMT	Epithelial-Mesenchymal Transition
GO	Gene Ontology
GSEA	Gene Set Enrichment Analysis
MDSC	Myeloid-derived suppressor cells
NK	Natural Killer cells
NSG	NOD Scid gamma mouse
PAGE	Polyacrylamide gel electrophoresis
PBS	Phosphate-buffered saline
PCR	Polymerase chain reaction
TBST	Tris Buffered Saline with Tween® 20
TCGA	The Cancer Genome Atlas
TF	Transcription factors
TIDE	Tumor Immune Dysfunction and Exclusion (TIDE)
TME	Tumor microenvironment
TIME	Tumor immune microenvironment
TNBC	Triple-negative Breast Cancer
UALCAN	University of Alabama at Birmingham CANcer data analysis Portal

Supplementary Information

The online version contains supplementary material available at <https://doi.org/10.1186/s12943-024-02102-y>.

Supplementary Material 1. Figure S1. NACC1 alteration in primary and metastatic samples in breast cancer samples. A) NACC1 genetic alterations in metastatic breast cancer samples. B) NACC1 genetic alterations in various primary breast cancer subtypes. C&D) NACC1 alterations subtypes in primary and metastatic samples. Figure S2. UALCAN-TCGA shows the association of NACC1 protein expression with altered oncogenic pathways in BC samples. A) NACC1 protein expression in BC samples ($n=125$) is higher than in adjacent normal tissues ($n=18$). B) NACC1 protein expression is higher in the tumors with alteration of the TP53/RB pathway ($n=81$) than in tumors without alteration of the TP53/RB pathway ($n=33$). Tumor samples without TP53/RB are labelled others in the graph. C) Expression of NACC1 protein is higher in the tumors with c-MYC alteration ($n=55$) than

those without c-MYC alteration (others, $n=55$). A total of 114 tumor samples and 18 normal samples were analyzed for TP53/RB alteration while 110 tumor samples and 18 normal tissues were analyzed for c-MYC alterations. Figure S3. Clinical relevance of NAC1 expression in breast cancer samples. A) Association of NAC1 expression with the overall survival of patients with HER2-positive BC, as shown by analysis of the TIDE database. B) Association of NAC1 expression with the overall survival of patients with luminal B breast cancer, as shown by analysis of the TIDE database. C) Association of NAC1 expression with the overall survival of patients with luminal A breast cancer, as shown by analysis of the TIDE database. D) Association of NAC1 promoter methylation with the overall survival of patients with breast cancer, as shown by analysis of the TIDE database. E) CD44 expression in MDA-MB-231 cells with or without knockdown of NAC1, as shown by immunofluorescence confocal microscopy. F) Aldolase activity in MDA-MB-231 cells with or without knockdown of NAC1. Figure S4. Altered gene expressions associated with NAC1 depletion in MDA-MB-231 cells. A) Volcano plot of DEGs of MDA-MB-231 cells with or without depletion of NAC1. B) Enrichment of cancer-associated genes and pathways in NAC1-deficient versus NAC1-expressing MDA-MB-231 cells. C–E) Expression of genes associated with CD44 expression and TNBC tumor progression in MDA-MB-231 cells with or without knockdown of NAC1. F) mRNA expression of ALDH1A3 in MDA-MB-231 cells with or without knockdown of NAC1. Figure S5. Effect of NAC1 expression on TNBC metastasis. A) Lung metastasis following the intravenous injection of EO771 cells with or without depletion of NAC1 (1×10^6 cells/inoculation). B) Lymph node metastasis of orthotopic MDA-MB-231 tumors ($n=2$). C) Illustration of the experimental procedure. D) Lung metastasis following orthotopic inoculation of EO771 cells in NAC1+/+ or NAC1-/- mice (1×10^6 cells/inoculation, $n=5$, $Tn=2$). E) Spontaneous lung metastasis of orthotopic MDA-MB-231 tumors with or without depletion of NAC1 in NSG mice (1×10^6 cells/inoculation, $n=5$, $Tn=2$). Figure S6. Analysis of DEGs in RNA seq data revealed the TFs associated with the NAC1-induced genes. A) Binding Analysis for regulation of transcription (BART) demonstrates STAT3 among highly implicated transcription factors (TFs) associated with NAC1 expression. B) BART reveals an association between the upregulated genes and EZH2 gene expression in the NAC1-deficient cells. C) BART TFs rank analysis demonstrates EZH2 as one of the top candidates in regulating NAC1-induced phenotype. D) Gene ontology analysis of NAC1-deficient tumor cells. E) Western blot analysis of RAB6A expression in NAC1-deficient tumor cells. Figure S7. Comparison of tumorigenicity of NAC1-expressing and NAC1-deficient TNBC cells in nude and NSG mice. A) Tumorigenicity of MDA-MB-231 cells in nude mice. B) Tumorigenicity of MDA-MB-231 cells in NSG mice (1×10^6 cells/inoculation, $n=4$, $Tn=4$). C) The in vivo limiting-dilution assay showing the tumorigenicity of MDA-MB-231 cells with or without depletion of NAC1 in NSG mice. D) Imaging of inoculated tumor cells at day 0. Figure S8. NK cells depletion in Balb/c mice. A) Confirmation of Nac1 depletion in mouse breast cancer 4T1 cells. A&C. Analysis of antibody depletion efficiency in Balb/C mice after GM1 antibody treatment

Supplementary Material 2.

Acknowledgements

We thank the Shared Resource Facility of the University of Kentucky and Markey Cancer Center (P30CA177558), the Imaging Core Facility of the Center for Cancer Metabolism COBRE (P20 GM121327), and UK histology core (ADC grant P30 AG072946) for technical support and assistance. We also thank Prof. Christine Brainson for her assistance with the artificial intelligence analysis, Mr. Leif Magnuson for his help with confocal microscopy imaging, and Dr. Sara Bachert and Ms. Dana Napier for their support in clinical sample identification and tissue slide processing.

Authors' contributions

Conceptualization, C.M.N., J.-M.Y., J.S. and X.L.; Methodology: C.M.N., R.S., J.K.; Y.Z.; X.X.; D.L.; Y.P.; Validation: C.M.N., F.O., A.S.; S.B.; Investigation: C.M.N., R.S., H.J.; J.K.; X.R.; H.H.; N.V.; B.Z.; S.B.; and J.S.; J.W.; Resources, J.-M.Y., J.S., and X.L.; Writing original draft preparation, C.M.N., J.-M.Y., and X.L., reviewing and editing, C.M.N.; X.R.; N.V.; B.Z.; J.W.; J.S.; X.L.; J.M.Y.; Funding acquisition, J.-M.Y., J.S., and X.L. All authors have read and agreed to the publication of this manuscript.

Funding

This work was supported by the National Cancer Institute Grant R01CA221867 to J.Y. and J.S., start-up funds from the Markey Cancer Center and College of Medicine, University of Kentucky, to J.Y., and Susan G. Komen Foundation CCR18548501 and NIH grant P20GM121327 to X.L.

Availability of data and materials

No datasets were generated or analysed during the current study.

Declarations

Ethics approval and consent to participate

All animal experiments were approved by the IACUC Committee of the University of Kentucky and were in concordance with the Animal Welfare Act, the Public Health Service policy on humane care and use of animals, the U.S. Government Principles for the utilization and care of vertebrate animals used in testing, research and training, and the NIH guide for the Care and Use of Laboratory Animals.

Competing interests

The authors declare no competing interests.

Received: 2 February 2024 Accepted: 27 August 2024

Published online: 06 September 2024

References

- Cha XY, et al. NAC-1, a rat brain mRNA, is increased in the nucleus accumbens three weeks after chronic cocaine self-administration. *J Neurosci*. 1997;17(18):6864–71.
- Wang J, et al. A protein interaction network for pluripotency of embryonic stem cells. *Nature*. 2006;444(7117):364–8.
- Kim J, et al. An extended transcriptional network for pluripotency of embryonic stem cells. *Cell*. 2008;132(6):1049–61.
- Malleshaiah M, et al. NAC1 Coordinates a Sub-network of Pluripotency Factors to Regulate Embryonic Stem Cell Differentiation. *Cell Rep*. 2016;14(5):1181–94.
- Yap KL, et al. Loss of NAC1 expression is associated with defective bony patterning in the murine vertebral axis. *PLoS ONE*. 2013;8(7):e69099.
- Nakayama K, et al. A BTB/POZ protein, NAC-1, is related to tumor recurrence and is essential for tumor growth and survival. *Proc Natl Acad Sci U S A*. 2006;103(49):18739–44.
- Nakayama K, et al. Homozygous deletion of MKK4 in ovarian serous carcinoma. *Cancer Biol Ther*. 2006;5(6):630–4.
- Yeasmin S, et al. Expression of the bric-a-brac tramtrack broad complex protein NAC-1 in cervical carcinomas seems to correlate with poorer prognosis. *Clin Cancer Res*. 2008;14(6):1686–91.
- Shih IM, et al. Amplification of the ch19p13.2 locus in ovarian high-grade serous carcinoma. *Mod Pathol*. 2011;24(5):638–45.
- Nakayama K, et al. Biological role and prognostic significance of NAC1 in ovarian cancer. *Gynecol Oncol*. 2010;119(3):469–78.
- Nakayama K, et al. NAC-1 controls cell growth and survival by repressing transcription of Gadd45GIP1, a candidate tumor suppressor. *Cancer Res*. 2007;67(17):8058–64.
- Jinawath N, et al. NAC-1, a potential stem cell pluripotency factor, contributes to paclitaxel resistance in ovarian cancer through inactivating Gadd45 pathway. *Oncogene*. 2009;28(18):1941–8.
- Tsunoda K, et al. Nucleus accumbens-associated 1 contributes to cortactin deacetylation and augments the migration of melanoma cells. *J Invest Dermatol*. 2011;131(8):1710–9.
- Zhang Y, et al. NAC1 modulates sensitivity of ovarian cancer cells to cisplatin by altering the HMGB1-mediated autophagic response. *Oncogene*. 2012;31(8):1055–64.
- Zhang Y, et al. Dysfunction of nucleus accumbens-1 activates cellular senescence and inhibits tumor cell proliferation and oncogenesis. *Cancer Res*. 2012;72(16):4262–75.
- Yap KL, et al. NAC1 is an actin-binding protein that is essential for effective cytokinesis in cancer cells. *Cancer Res*. 2012;72(16):4085–96.

17. Ueda SM, et al. Expression of Fatty Acid Synthase Depends on NAC1 and Is Associated with Recurrent Ovarian Serous Carcinomas. *J Oncol*. 2010;20(10): 285191.
18. Cerami E, et al. The cBio cancer genomics portal: an open platform for exploring multidimensional cancer genomics data. *Cancer Discov*. 2012;2(5):401–4.
19. Li TW, et al. TIMER2.0 for analysis of tumor-infiltrating immune cells. *Nucleic Acids Res*. 2020;48(W1):W509–14.
20. Chen F, et al. Polycomb deficiency drives a FOXP2-high aggressive state targetable by epigenetic inhibitors. *Nat Commun*. 2023;14(1):336.
21. Olofsen, P.A., et al., Effective, Long-Term, Neutrophil Depletion Using a Murinized Anti-Ly-6G 1A8 Antibody. *Cells*, 2022;11(21).
22. Dean I, et al. Rapid functional impairment of natural killer cells following tumor entry limits anti-tumor immunity. *Nat Commun*. 2024;15(1):683.
23. Li P, et al. Dual roles of neutrophils in metastatic colonization are governed by the host NK cell status. *Nat Commun*. 2020;11(1):4387.
24. Lin Q, et al. IFN-gamma-dependent NK cell activation is essential to metastasis suppression by engineered Salmonella. *Nat Commun*. 2021;12(1):2537.
25. Wu SZ, et al. A single-cell and spatially resolved atlas of human breast cancers. *Nat Genet*. 2021;53(9):1334–47.
26. Marimuthu S, et al. Mucins reprogram stemness, metabolism and promote chemoresistance during cancer progression. *Cancer Metastasis Rev*. 2021;40(2):575–88.
27. Kessenbrock K, Wang CY, Werb Z. Matrix metalloproteinases in stem cell regulation and cancer. *Matrix Biol*. 2015;44–46:184–90.
28. Zhu Y, et al. High expression of syndecan-4 is related to clinicopathological features and poor prognosis of pancreatic adenocarcinoma. *BMC Cancer*. 2022;22(1):1042.
29. Karagiorgou, Z., et al., Proteoglycans Determine the Dynamic Landscape of EMT and Cancer Cell Stemness. *Cancers (Basel)*, 2022;14(21).
30. Qiu GZ, et al. Reprogramming of the Tumor in the Hypoxic Niche: The Emerging Concept and Associated Therapeutic Strategies. *Trends Pharmacol Sci*. 2017;38(8):669–86.
31. Bayik D, Lathia JD. Cancer stem cell-immune cell crosstalk in tumour progression. *Nat Rev Cancer*. 2021;21(8):526–36.
32. Chen J, et al. The development and improvement of immunodeficient mice and humanized immune system mouse models. *Front Immunol*. 2022;13:1007579.
33. Razi S, et al. The role of tumor microenvironment on cancer stem cell fate in solid tumors. *Cell Commun Signal*. 2023;21(1):143.
34. Li YR, et al. Exploring the dynamic interplay between cancer stem cells and the tumor microenvironment: implications for novel therapeutic strategies. *J Transl Med*. 2023;21(1):686.
35. Ngule, C.M., et al., Identification of a -Regulated Gene Signature Implicated in the Features of Triple-Negative Breast Cancer. *Biomedicines*, 2023;11(4).
36. Reya T, et al. Stem cells, cancer, and cancer stem cells. *Nature*. 2001;414(6859):105–11.
37. Battle E, Clevers H. Cancer stem cells revisited. *Nat Med*. 2017;23(10):1124–34.
38. Liu X, et al. EGFR inhibition blocks cancer stem cell clustering and lung metastasis of triple negative breast cancer. *Theranostics*. 2021;11(13):6632–43.
39. Liu X, et al. Homophilic CD44 Interactions Mediate Tumor Cell Aggregation and Polyclonal Metastasis in Patient-Derived Breast Cancer Models. *Cancer Discov*. 2019;9(1):96–113.
40. Liu H, et al. Cancer stem cells from human breast tumors are involved in spontaneous metastases in orthotopic mouse models. *Proc Natl Acad Sci U S A*. 2010;107(42):18115–20.
41. Lawson DA, et al. Single-cell analysis reveals a stem-cell program in human metastatic breast cancer cells. *Nature*. 2015;526(7571):131–5.
42. Al-Hajj M, et al. Prospective identification of tumorigenic breast cancer cells. *Proc Natl Acad Sci U S A*. 2003;100(7):3983–8.
43. Prasetyanti PR, Medema JP. Intra-tumor heterogeneity from a cancer stem cell perspective. *Mol Cancer*. 2017;16(1):41.
44. Liu Y, et al. NAC1/HMGB1 Signaling Pathway Is Associated with Epithelial-mesenchymal Transition, Invasion, and Metastasis of Lung Cancer Cell Line. *Ann Clin Lab Sci*. 2018;48(5):559–64.
45. Zhang Y, et al. Nucleus accumbens-associated protein-1 promotes glycolysis and survival of hypoxic tumor cells via the HDAC4-HIF-1 α axis. *Oncogene*. 2017;36(29):4171–81.
46. Ma T, et al. The C-terminal pentapeptide of Nanog tryptophan repeat domain interacts with NAC1 and regulates stem cell proliferation but not pluripotency. *J Biol Chem*. 2009;284(24):16071–81.
47. Faiola F, et al. NAC1 Regulates Somatic Cell Reprogramming by Controlling Zeb1 and E-cadherin Expression. *Stem Cell Reports*. 2017;9(3):913–26.
48. Lee JL, Wang MJ, Chen JY. Acetylation and activation of STAT3 mediated by nuclear translocation of CD44. *J Cell Biol*. 2009;185(6):949–57.
49. Honeth G, et al. The CD44+/CD24- phenotype is enriched in basal-like breast tumors. *Breast Cancer Res*. 2008;10(3):R53.
50. Ma F, et al. Enriched CD44(+)/CD24(-) population drives the aggressive phenotypes presented in triple-negative breast cancer (TNBC). *Cancer Lett*. 2014;353(2):153–9.
51. Kim IS, et al. Immuno-subtyping of breast cancer reveals distinct myeloid cell profiles and immunotherapy resistance mechanisms. *Nat Cell Biol*. 2019;21(9):1113–26.
52. Li L, Jensen RA. Understanding and Overcoming Immunosuppression Shaped by Cancer Stem Cells. *Cancer Res*. 2023;83(13):2096–104.
53. Maas RR, et al. The local microenvironment drives activation of neutrophils in human brain tumors. *Cell*. 2023;186(21):4546–4566e27.
54. Neophytou CM, et al. The Role of Tumor-Associated Myeloid Cells in Modulating Cancer Therapy. *Front Oncol*. 2020;10:899.
55. Miranda A, et al. Cancer stemness, intratumoral heterogeneity, and immune response across cancers. *Proc Natl Acad Sci U S A*. 2019;116(18):9020–9.
56. Pang, L., et al., Kunitz-type protease inhibitor TFPI2 remodels stemness and immunosuppressive tumor microenvironment in glioblastoma. *Nat Immunol*, 2023.
57. Liu Y, et al. Cell Softness Prevents Cytolytic T-cell Killing of Tumor-Repopulating Cells. *Cancer Res*. 2021;81(2):476–88.
58. Meyer C, et al. Frequencies of circulating MDSC correlate with clinical outcome of melanoma patients treated with ipilimumab. *Cancer Immunol Immunother*. 2014;63(3):247–57.
59. Ostrand-Rosenberg S, Fenselau C. Myeloid-Derived Suppressor Cells: Immune-Suppressive Cells That Impair Antitumor Immunity and Are Sculpted by Their Environment. *J Immunol*. 2018;200(2):422–31.
60. Highfill SL. Disruption of CXCR2-mediated MDSC tumor trafficking enhances anti-PD1 efficacy. *Sci Transl Med*. 2014;6(237):237ra67.
61. De Henau O, et al. Overcoming resistance to checkpoint blockade therapy by targeting PI3Kgamma in myeloid cells. *Nature*. 2016;539(7629):443–7.
62. Kim K, et al. Eradication of metastatic mouse cancers resistant to immune checkpoint blockade by suppression of myeloid-derived cells. *Proc Natl Acad Sci U S A*. 2014;111(32):11774–9.
63. Kaczanowska, S., et al., Genetically engineered myeloid cells rebalance the core immune suppression program in metastasis. *Cell*, 2021.
64. Sharma P, et al. The Next Decade of Immune Checkpoint Therapy. *Cancer Discov*. 2021;11(4):838–57.
65. Blayney DW, Schwartzberg L. Chemotherapy-induced neutropenia and emerging agents for prevention and treatment: A review. *Cancer Treat Rev*. 2022;109: 102427.

Publisher's Note

Springer Nature remains neutral with regard to jurisdictional claims in published maps and institutional affiliations.